8-2013

The Development of a Rapid Fiber-Based Immunoassay as a Point-of-Care or In-Home Diagnostic Test

Christopher Waddell
Clemson University, c.ryan.waddell@gmail.com

THE DEVELOPMENT OF A RAPID FIBER-BASED IMMUNOASSAY AS A POINT-OF-CARE OR IN-HOME DIAGNOSTIC TEST

A Thesis
Presented to
the Graduate School of
Clemson University

In Partial Fulfillment
of the Requirements for the Degree
Master of Science
Bioengineering

---

by
Christopher Ryan Waddell
August 2013

Accepted by:
Dr. Alexey Vertegel, Committee Chair
Dr. Konstantin Kornev
Dr. Agneta Simionescu

Abstract

Early diagnosis of conditions allows for physicians to treat patients earlier, and ultimately improve patient outcomes. Two conditions of particular interest for earlier and cheaper diagnosis are the influenza virus and human immunodeficiency virus (HIV). Antiviral treatment administered within the first 48 hours of influenza infection decreases symptom severity, risk of complications, and reduced healthcare costs. Early diagnosis of HIV can decrease the risk of transmission of the virus to HIV negative individuals and allow for earlier administration of highly active antiretroviral treatment (HAART), improving patient quality of life and patient outcomes.

Currently, the "gold standard" for detection of both Influenza and HIV are tests performed in a clinical laboratory setting. There are rapid diagnostic tests that can be performed at the point-of-care or an in-home setting, but these tests have their limitations. This study aims to develop a highly sensitive, nanofiber-based immunochromatography assay for the detection of such conditions at the point-of-care or an in-home setting. Electrospun CA/PMMA/PEO nanofiber yarns were prepared and shown to be a viable substrate for antibody attachment and detection of conditions. Colloidal gold-labeled antibodies were prepared to detect analyte in a solution, allowing for detection of an analyte visible to the naked eye. Furthermore, several immunoassay systems were successfully developed using each of these components. These immunoassay systems have potential for employment either at the point-of-care or as in-home diagnostic tools to allow for earlier diagnosis.

Dedication

I would like to dedicate this work to my family and friends for their guidance and unwavering support throughout my life. They have been instrumental in my personal growth development as well as aiding all my achievements.

Acknowledgements

Endless gratitude to my advisor, Dr. Alexey Vertegel, for all his guidance and help with my research and professional and academic development over the past several years during my undergraduate and graduate career at Clemson University. All of his time, effort, and interest are truly appreciated. I would like to thank Dr. Konstantin Kornev for the many constructive discussions and new perspectives he and his lab group have provided throughout our collaboration. It has been a key element in the progression of my research. I would also like to thank Dr. Agneta Simionescu for all her consideration and interest in my research, as well as furthering my undergraduate and graduate academic development. I would like to specifically thank her, along with Mrs. Linda Jenkins, for her help with immunohistochemistry techniques. Heartfelt thanks to Dr. Vladimir Reukov and Dr. Aleksey Shaporev for all their guidance and mentorship throughout my research. I would also personally like to show my appreciation to all the past and present members of the Bionanomaterials Lab who have provided me so much support and assistance throughout my undergraduate and graduate research, especially Dr. Victor Maximov for his aid with my fiber-based research. Special thanks go to Dr. Chen-Chih Tsai of Dr. Kornev's group for the preparation of the numerous fibers necessary for my research. Thanks also go to Olga Reukova for her help with the design of Figure 9. I would also like to thank Dr. Melinda Harman and her lab, especially Ryan Freed, for help with the interferometer measurements. Finally, I would like to thank Dr. Martine LaBerge and all the faculty and staff of the Department of Bioengineering for their aid in my academic and professional development.

Table of Contents

Page

List of Tables

Table **Page**

List of Figures

Figure **Page**

Chapter 1

Introduction

Early diagnosis of conditions allows physicians to better and more accurately treat patients to improve patient outcomes [1]. For patients infected with the influenza virus, earlier antiviral treatment, within the first 48 hours, leads to decreased symptom severity and risk of complications [2-4]. The conventional "gold standard" for influenza diagnosis is viral cell culture [5-8]. This diagnostic method; however, requires a long turn-around time and its complexity requires it to be performed in a clinical laboratory setting rather than at the point-of-care. More recently, rapid influenza diagnostic tests (RIDTs) have gained traction for diagnosis of influenza at the point-of-care [5-9]. However, the sensitivity of these tests is lacking in some cases and they are not employed for an in-home diagnostic setting [10-13].

Human immunodeficiency virus (HIV) is a serious and chronic viral infection. Like influenza, early highly active antiretroviral treatment (HAART) administration improves patients' quality of life, longevity, and reduces the risk of virus transmission [14-17]. The "gold standard" for HIV diagnosis is the HIV enzyme immunoassay (EIA) [14]. However, this methodology requires a long turn-around time for results, has a high complexity requiring testing in a clinical laboratory setting, and may give false negative

results at certain time-points. These diagnostic tests also incur high costs that limit availability to those in low-resource settings [14, 16, 18-20]. There are several rapid HIV diagnostic tests currently available, one of which has been approved for in-home use by the patient.

Chapter 2 begins by providing a brief overview of immunology, specifically the immune system, antibody structure, function, and interaction with biomolecules. The influenza virus and treatment are then briefly discussed, followed by an overview of current diagnostic testing approaches. Clinical and financial considerations of the human immunodeficiency virus are then discussed along with current HIV testing strategies. Finally, a review of diagnostic testing methodologies is presented, including a brief explanation of the clinical laboratory improvement amendments law (CLIA). The principles of immunoassays, employed in immunochromatography, fluorescence immunoassays and immunohistochemistry, are reviewed along with other clinical laboratory diagnostic methods. The literature review concludes mentioning in-home diagnostic tests that are currently available.

Electrospun polymeric nanofiber yarns have been shown to have high specific surface area, useful for surface modification and use in various fields, including biosensor applications. Chapter 3 discusses the preparation and functionalization of electrospun nanofiber yarns for employment in an immunoassay system. Current over-the-counter diagnostic tests apply the immunochromatography principle using gold nanoparticles to provide the signal read by the end-user. The preparation and characterization of colloidal

gold-labeled antibodies for use as an optical label for analytes is presented in Chapter 4, followed by the development of an immunochromatographic assay utilizing the aforementioned yarns and gold-labeled antibodies. The functionalized yarns and colloidal gold-labeled antibodies are then employed in several configurations of immunochromatographic assays in Chapter 5. Chapter 6 summarizes the findings of this study and provides further recommendations for continuation of the research.

Chapter 2

Literature Review

2.1 Immunology: A Brief Overview

2.1.1 The Immune System

The immune system defends the body from foreign invaders utilizing two subsystems: innate immunity and acquired immunity. The body's innate immunity is derived from general mechanisms that prevent pathogens from entering or thriving in the body. The protection offered by the skin as a physical barrier, the acidic pH of the stomach and enzymes that breakdown foreign substances are examples of components that make up the body's innate immunity. Acquired immunity arises due to exposure to specific stimuli.

Acquired immunity can be further broken down into cell-mediated immunity and humoral immunity. Cell-mediated immunity begins with the recognition of an antigen by T cells which leads to downstream cytotoxic activity, by cytotoxic T cells, and chemical regulation of the body's immune response, by helper T cells. The lymphokines, secreted by helper T cells, and direct antigen interaction with cell membrane immunoglobulins activates the B cells responsible for humoral immunity. Activated B cells differentiate into memory B cells and plasma cells. Memory B cells are produced to quickly respond to antigen presentation in the future. Plasma cells' high-functioning and extensive rough

endoplasmic reticulum enables this cell type to excrete large quantities of antibodies with variable portions that are reactive with the antigen initializing the immune response. Plasma cells are capable of secreting up to 2,000 antibody molecules per second. This high antibody production rate may continue on a time scale of days to weeks [21, 22]. The antibodies produced by these plasma cells are a key component in the body's defense against foreign invaders.

2.1.2 Antibody Structure and Function

The term antibody is used to generalize five different classes of immunoglobulins, which are glycoproteins that can be found in the cell membranes of B cells or in body fluids. It is important to note that the physiological distribution, function, and structure of immunoglobulins vary from class to class. Plasma immunoglobulins are dominated by Immunoglobulin G (IgG), which composes 80% of immunoglobulins found in serum, at about 12.5 mg/ml. The main immunoglobulin in saliva, nasal secretions, bronchial secretions, tears, and colostrum is immunoglobulin A (IgA). It is primarily secreted in mucosal membranes to defend against microorganisms, but can also be found in small quantities in serum. Also found in serum, composing 10% of immunoglobulins there, is the immunoglobulin M (IgM) class antibody. Allergic reactions are facilitated by immunoglobulin E-antigen interactions. These physiological distributions and functions are important to antibody employment in the development of immunoassays [21, 23]. The structure of antibodies varies among the immunoglobulin classes and is related to function and physiological location. For instance, IgM exists as a pentameric molecule

and serum IgA can exists as a monomers, dimers, or trimers in secretions while secretory IgA is a dimer that includes a secretory component [24]. A schematic of the basic structure of an immunoglobulin G, or IgG, molecule is shown in Figure 1.

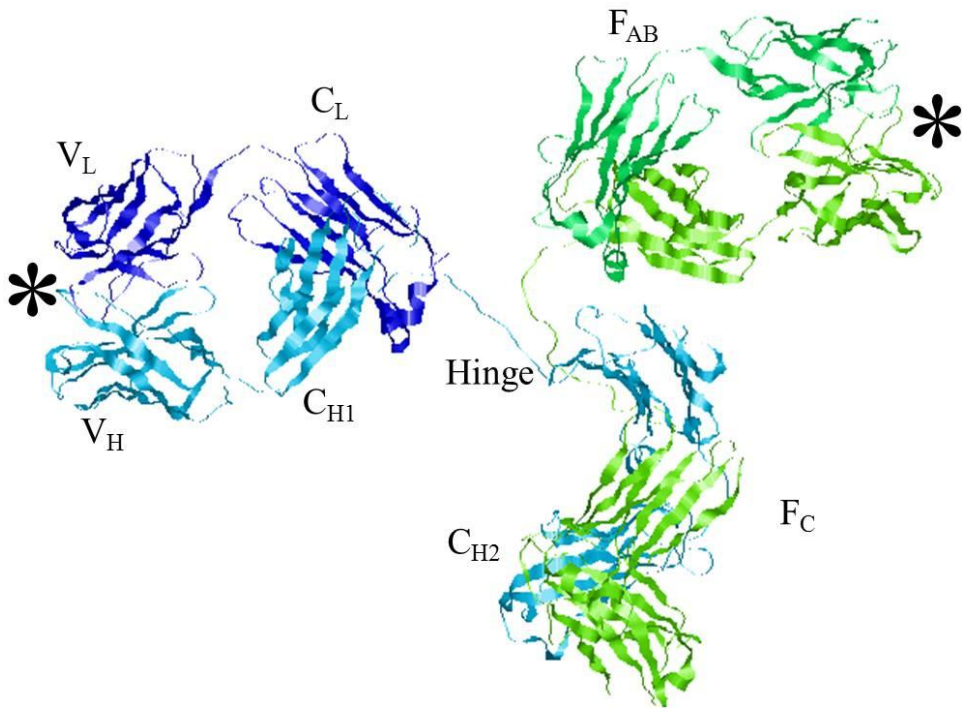

Figure 1. The protein ribbon structure of an IgG (2a) monoclonal antibody as determined by X-ray diffraction. Shown here are the heavy chains (light green and light blue) and the light chains (dark blue and dark green). Shown are the variable regions of the heavy and light chains (V_H and V_L), the constant region of the light chain (C_L) and heavy chains (C_{H1} and C_{H2}), the hinge, and the F_{AB} and F_C regions. Also visible is the antigen binding sites (*) between the heavy and light chains. File downloaded from the protein data bank, PDB ID: 1IGT [25, 26].

Immunoglobulin G molecules (150 kDa) are made up of two heavy chains (50 kDa) each linked to a light chain (23 kDa) via disulfide bonds and non-covalent interactions

[25, 27, 28]. The two F_{ab} regions are composed of the variable regions of light chains (V_L) paired with variable regions of heavy chains (V_H) and the constant regions of the light chains (C_L) paired with a part of the constant portion of the heavy chain (C_{H1}). Generally, the F_{ab} region of an immunoglobulin is composed of 2 beta-sheets closely packed and covalently linked by disulfide bridges in the constant region [28]. The pairing of the V_L and V_C regions is where the specific antigen-antibody reactions occur. The variable region can be further divided into the framework amino acid sequences and hyper-variable regions, also referred to as complementarity-determining regions (CDRs). The framework sequences provide structure to the protein and position the CDRs properly to allow for antigen binding. The antigen binding sites are formed between the heavy and light chain variable segments where the CDRs reside [23, 25, 27, 28]. The pairing of the heavy chains constant portion (C_{H2a} and C_{H2b}) is referred to as the F_C region. The F_c region amino acid sequence contains the carboxyl group terminal end.

Antibodies can be produced that are either polyclonal, with the ability to recognize several different epitopes, or monoclonal, recognizing only one epitope. Fixation and denaturation of proteins usually does not destroy all epitopes that may be recognized by polyclonal antibodies. The ability to recognize and react with several epitopes allows polyclonal antibodies to be used on such processed samples as fixed tissue, for immunohistochemical applications. In contrast, monoclonal antibodies are much more sensitive to modifications. This may lead to non-reactive antigen binding moieties due to epitope masking under different conditions [29]. The interactions between antibodies and

their antigens need to be explored further to illustrate the functionality of antibodies, both physiologically and for potential diagnostic applications.

2.1.2 Antibody-Antigen Interactions

All antibody-antigen complexes have a high affinity [25, 28]. These antigen-antibody reactions are characteristically different, depending on the type of antigen, whether the antigen is a protein, antibody, carbohydrate, or peptide. The protein antigen-F_{ab} interface has high morphological complementarity, with hydrogen bonds, salt bridges and van der Waals forces acting at the interface. These protein antigen-antibody interactions have reported K_a values of 10^7-10^{10} M^{-1} [28]. Studies have shown that hydrophobic interactions between antibodies and small molecules have had the highest correlation with analyte binding. Other factors that influence the binding include electrical and steric properties of analytes [30]. These antibody-antigen interactions provide the basis for many diagnostic tests and tools in a variety of fields. Other than diagnostic tests, antibodies have been used to study the physiological response to biomaterials [31-37], as well as in therapeutic applications [38, 39].

Antibodies not only mediate the interaction of antigens with cells, they can also neutralize the harmful effects of antigens directly via two separate mechanisms: agglutination and masking key epitopes [21, 38, 40]. The agglutination resulting from antibody-antigen interactions can be dramatic enough to precipitate soluble antigens out of solution into a state where they are inactive [21, 40]. Of particular interest for this study is the interaction between antibodies and influenza virus neuraminidase [3, 28, 40,

41]. These antibody-antigen interactions inhibit neuraminidase and hemagglutinin activity of the antigen [40].

Both monoclonal and polyclonal antibodies have been shown effective in prophylactic and therapeutic use in vaccines. Antibodies' antiviral properties arise from the highly specific epitope binding mechanism. Antibodies can prevent virus entrance into a cell by binding viral spikes, cell receptors or co-receptors, inducing cell or endosomal membrane conformational changes, agglutination of virus, and inhibiting viral product release [38-45].

The response by the immune system acts primarily to respond to the specific stimuli encountered; however, it may also disclose information regarding the type of invasive pathogen or infection. The antibodies produced respond as described above and are found at elevated levels in tissues and body fluids, depending on the antibody type. The elevated level of antibodies and biomolecules in clinical samples provides target analytes to be probed and analyzed by biosensors to aid physicians in diagnosing the pathogen or infective agent present. The physiological response, especially antibodies and antigens, has been employed in the diagnosis of several conditions, including influenza and human immunodeficiency virus.

2.2 Current Strategies for detecting conditions

Antibody-antigen interactions can be extremely useful in determining the presence of a pathogen. Understanding these antibody-antigen interactions has allowed for the development of immunoassays that are commonly used to detect a variety of conditions

in every diagnostic testing setting: histology and clinical laboratories, point-of-care settings, and in-home diagnostics. A sound understanding of immunoassay principles allows for the assessment and comparison of current and prospective technologies for advancement of diagnostics.

2.2.1 Immunoassay Principles

Immunoassays employ the inherent sensitivity, specificity, and binding affinities of antibodies to respective antigens to detect the presence of antigen in a sample. Samples typically tested include whole blood, plasma, serum, saliva, and respiratory fluids. Immunoassay signals typically come from the accumulation of a labeled antibody at the binding site for the antigen on a substrate. Typical antibody labels may be fluorescent molecules, nano- or microparticles, or enzymes. These immunoassays can be employed in industry, clinical or laboratory settings, doctor's offices, or as over-the-counter tests. Over-the-counter tests typically utilize the immunochromatography technique with antibody labels that can be seen by the naked eye, such as gold nanoparticles or latex beads [46, 47].

2.2.2 Immunohistochemistry

Histology is the study of tissue structure and function. Sections of tissues are taken and stained with specialized stains to show different cells, structures, and compounds present in the sample. Clinical histology can be taken from patients to aid in the diagnosis of various conditions in patients. Histology has also been employed in the field of bioengineering to examine the effects of medical devices, surgical techniques,

and other therapeutics administered to animal specimens. One histological tool that has been found to be particularly useful is immunohistochemical staining. Immunostaining of cells or cellular structures can be performed with antibodies labeled with an enzyme, such as horseradish peroxidase (HRP), or fluorescent labels, that will reveal antibody locations after chemical reaction or excitation by specific wavelengths, respectively [36, 37, 48-52]. Traditionally histology is used in hospital or clinical laboratory settings to aid in the diagnosis of various conditions. More recently it has been found useful in the analysis of the physiological response to implanted biomaterials [31-37]. This principle, using the specific and sensitive reactions of antibodies and antigens, can be adapted and used to detect antibody presence on nanofiber yarns, as well as specific reactivity of immobilized antibody on nanofiber yarns. The same interactions can be applied to some clinical laboratory diagnostic tests.

2.2.3 Laboratory Analysis

There are several diagnostic tests methodologies that provide excellent sensitivity, such as enzyme immunoassays (EIAs) and viral cell cultures currently used for the diagnosis of HIV and influenza, respectively. Other methods include polymerase chain reaction (PCR) and enzyme-linked immunosorbent assay (ELISA). While these techniques offer exceptional sensitivities, they do require technical knowledge and expertise. Also required for both of these methods is expensive equipment that may not be available at the point-of-care, and will certainly not be available for patients' self-diagnosis [11, 13, 53-56]. To illustrate the complexities that can be associated with these

methods a brief description of viral cell culture for influenza diagnosis and enzyme immunoassays for HIV follows.

2.2.3.1 Viral Cell Culture

There are various methods and tools available to clinicians to aid in the diagnosis of influenza. Conventionally, viral cell cultures are performed and considered the "gold standard" for virus diagnosis [5-8]. Specimens used in this method include Nasopharyngeal (NP) swabs, throat swab, NP or bronchial washes, nasal or endotracheal aspirate, and sputum [7]. A general procedure for collecting and analyzing specimens by viral cell culture is briefly described as follows: These specimens are collected with swabs made of Dacron or polyester, and then placed in special medium for transport to the laboratory. The viral transport medium (VTM) generally contains antibiotics necessary eliminate potential microbial contamination, buffer solution with pH indicator, and a protein source. The tube containing VTM and the sample collection swab is mixed thoroughly, and the swab is then removed. The VTM with sample is centrifuged to a pellet, containing cells, bacteria and other large particles, and supernatant. Due to their size, viruses are not spun down into the pellet. The virus-containing supernatant is collected and added to a cell culture or used to inoculate via adsorption inoculation. For adsorption inoculation, cell culture medium is discarded and the viral supernatant, or inoculation medium, is applied to the cell monolayer and incubated at 37°C for various time periods depending on the specimen type and viral infection of interest. The cells cultured with the inoculation medium are observed using a light microscope for

proliferation of the suspected virus. Expertise is required to recognize the effects of virus on the cell monolayer, especially for early or subtle changes. Changes in the cell culture due to viral infection, or cytopathic effects, can be seen for most viruses around 5-10 days post-inoculation. However, this time period varies depending on the virus type [7].

This time period for diagnosis can be reduced using more advanced methods of viral isolation. Viral inoculation can be enhanced by centrifugation-enhanced techniques. The processed sample is deposited directly onto a small coverslip that can fit into centrifugation tubes, after the VTM has been removed. Low centrifugal force is applied the vial and fresh culture medium is then added and the sample is incubated at 37°C. The coverslip with the clinical sample is subsequently stained with horseradish peroxidase (HRP) or fluorescently labeled antibodies. Examination with light microscopy (HRP-labeled antibodies) or fluorescent microscopy (fluorescently labeled antibodies), can reveal viral infection as early as 48 hours post-inoculation [5-7]. However, this rapid virus isolation technique increases diagnosis costs from equipment and reagents.

Despite the challenges presented by the turn-around time by the viral cell culture methods, samples must be transported to clinical laboratories under controlled conditions, special equipment and reagents are required in the clinical laboratory, and skilled technicians must perform the experiments. All these factors add to the cost and complexity of the diagnosis.

Antiviral regimens started after the first 48 hours have also been shown to reduce symptom and complication severity [2-4, 57]. This would help relieve some of the

financial burden of the influenza virus, which is especially important to those without sufficient resources and those without health insurance coverage. Those hospitalized by influenza could decrease their length of stay reducing the cost associated with the virus. Therefore, decreasing the turn-around time for patient diagnosis is important.

2.2.3.2 Enzyme Immunoassay

The current "gold standard" for HIV testing is an HIV enzyme immunoassay (EIA) for detection of HIV-1 and HIV-2 antibody presence with a western blot or immunofluorescence assay (IFA) to confirm the presence of HIV-1 antibody [14]. These tests can be performed with plasma or serum analytes. False negatives often result because although there is HIV infection present, the EIA may be non-reactive from 8-12 weeks post-infection. While these tests are sensitive, there is the need to send samples to a lab, increasing costs and turn-around time required to diagnose a patient [14, 58]. Enzyme immunoassays can also be performed on oral fluid specimens, which can be more convenient for collection. However, oral fluid samples for EIA still require sample transportation to a laboratory and are more expensive than traditional EIA techniques. The turn-around time for these samples is reduced to 3-5 business days [14]. Another advantage oral fluid specimens is that collection less invasive and hazardous to handle[58]. Enzyme immunoassays have proven effective in detecting the presence of HIV; however, this methodology is too complex to be used outside of clinical laboratory settings and, like viral cell culture, involves a long turn-around time.

2.2.4 Clinical Laboratory Improvement Amendments (CLIA)

Simplification of diagnostic testing methods allows for an increased availability of the diagnostic tests to patients with a shorter turn-around time. However, this simplification and increased availability must not detract from the reliability of the diagnoses. The Clinical Laboratory Improvement Amendments (CLIA) law specified that the complexity of tests should determine laboratory requirements. Diagnostic tests and assays are rated on their complexity by the FDA based on knowledge, training and experience required, reagent and material preparation, characteristics of operational steps, calibration, quality control, and proficiency testing materials, test system troubleshooting and maintenance, interpretation and judgment. The simplest diagnostic tests require little scientific or technical knowledge, where all required information can be learned on-site. Minimal training and experience should be required to conduct and analyze the results of the test. Reagents used in the tests should be stable and reliable, requiring no special handling, preparation, or storage conditions. The diagnostic test should also be operationally simple, preferably with automated steps. All calibration, quality control, and proficiency testing materials should be stable and readily available. Troubleshooting of the test system should be either automatic or self-correcting, or clearly described without experienced judgment required. Maintenance should also be provided by the manufacturer, rarely needed, or simple for the user. Importantly, there should be little room for judgment or interpretation error for analysis or resolution of problems [59]. Diagnostic tests that are CLIA waived, and therefore exempt from regulation, should be simple and accurate enough to ensure high probability of correct results [60].

There has recently been a shift toward the development of cheaper, CLIA-waived point-of-care diagnostic tools [8, 56]. These point-of-care diagnostics do not require the need for specialized and expensive equipment or extensively trained staff. The samples do not need to be specially handled and stored for transportation from the doctor's office to a clinical laboratory for analysis. The samples can also be analyzed by those on staff at the point-of-care, rather than specially trained clinical laboratory technicians. All these factors allow reduce the time and cost for diagnosis, enabling early treatment [5-9, 56]. The early treatment and increased availability for these CLIA-waived test is especially important for conditions such as influenza and HIV.

2.2.4.1 CLIA-waived Diagnostic Tests

The development of CLIA-waived influenza tests has been of particular interest due to the improvement in healthcare associated with earlier diagnosis. Rapid diagnostic influenza tests are listed with their sensitivities and specificities in Table 1.

Table 1. CLIA-waived RIDTs currently on the market along with specimens approved for CLIA-waived use along with the time to run the diagnostic test.

CLIA-waived RIDTs	Approved Specimens	Time
BD Veritor System for Rapid Detection of Flu A+B	NP swab/nasal swab	10 minutes
BinaxNOW® Influenza A&B	NP swab; Nasal wash/aspirate/swab	15 minutes
QuickVue® Influenza Test	nasal wash/aspirate/swab	10 minutes
QuickVue® Influenza A+B Test	NP swab; Nasal wash/aspirate/swab	10 minutes
SAS™ FluAlert A	Nasal wash/aspirate	15 minutes
SAS™ FluAlert B	Nasal wash/aspirate	15 minutes

It has been shown that nasopharyngeal samples have shown the highest sensitivity for sample collection in lateral-flow RIDTs, due to the availability of the antigen [11, 61-65]. While RIDTs can provide a convenient method to detect the presence of influenza antigens, it has been shown that some RIDTs offer lower sensitivity compared to the "gold standard" for influenza diagnostic tests [11, 61, 66]. There are RIDTs available that allow for detection of analyte in the nanogram range [8, 62]. However, when compared to RT-PCR tests, commercially available RIDTs result in decreased clinical sensitivity (70-90% in children and <40-60% in adults). Thus, it is recommended to confirm negative results via RT-PCR or viral cell culture [65]. Another concern is the variability of sensitivities that have been found in studies comparing RIDTs to RT-PCR. For the same commercially available RIDT, studies from different investigators have shown values for the sensitivity from 20% [11, 12] to 53.3% [10, 11]. Not only are these commercially available RIDTs lacking in sensitivity, with some shown to be as little as 9.7% sensitive [13], there is also variability and large amounts of inconsistencies with different users [11].

Some RIDTs are categorized as CLIA-waived tests, which facilitate the ease of use as point-of-care diagnostics. However, RIDTs are not available for over-the-counter testing, largely due to the discomfort associated with collecting the nasopharyngeal samples with higher antigen availability. Thus, there exists a need for the development of a highly sensitive RIDT that will cause less discomfort for patients and could possibly be used as an in-home diagnostic tool after an affordable over-the-counter purchase.

The benefits of earlier diagnosis of HIV have also drawn attention for CLIA-waived tests for this virus. CDC recommendations for HIV testing have been put forth and altered over the years. These recommendations are based on individuals' risk of contracting the virus, with higher risk patients testing more frequently than lower risk individuals. The latest CDC recommendation, from 2006, is that low risk individuals get tested once for HIV, while those at high risk receive annual testing [14, 18, 67, 68]. A study by Lucas, et al, showed testing for HIV more frequently and earlier administration of HAART is actually more effective in terms of dollars per quality-adjusted life-years (QALY). This study recommended HIV testing every three months for those at high risk of contracting HIV, giving an incremental cost effectiveness of $45,074/QALY [67].

It has been shown and is widely accepted by clinicians that early diagnosis of HIV decreases the chance for transmission of the disease and allows for administering highly active antiretroviral treatment, or HAART, earlier increasing quality of life, survival rates and patient longevity [14-17]. Testing for HIV more frequently reduces the risk for transmission of the disease and allows for early antiretroviral treatment, improving patient outcomes [14-16].

The FDA has approved 6 rapid HIV diagnostic tests that are commercially available in the United States: OraQuick® Rapid HIV-1/2 Antibody Test (OraSure Technologies, Inc.), Reveal G3 Rapid HIV-1 Antibody Test (MedMira, Inc.), Uni-Gold Recombigen HIV Test (Trinity BioTech), Multispot HIV-1/HIV-2 Rapid Test (Bio-Rad Laboratories), Clearview HIV 1 / 2 Stat PaK and Clearview Complete HIV 1 / 2

(Inverness Medical Professional Diagnostics). Each CLIA-waived HIV test requires whole blood, with the exception of the OraQuick® tests, which can also use saliva samples.

These rapid tests require confirmation for reactive (preliminary positive) results and repeat testing for invalid results. A major advantage of these rapid tests is that they can be used in point-of-care settings and results can be obtained within 10-30 minutes. This is especially important in low resource settings such as correctional facilities and low-income areas [69-71]. While these rapid tests incur higher material cost than traditional HIV testing, the cost per HIV-infected patient test result was lower, as confirmatory EIA and western blots are not required for non-reactive rapid test results [14, 58].

In 2012, the first over-the-counter HIV test for at-home use gained pre-market approval from the FDA. The OraQuick® In-Home HIV Test was derived from the OraQuick® Advance HIV-1/2 Antibody Test. Phase III clinical studies of the OraQuick® In-Home HIV Test yielded a sensitivity of 91.7% [72]. The OraQuick® In-Home HIV costs $39.99 per test kit. There exists a need to reduce the cost of these in-home tests, to increase availability to patients with minimal resources. This is especially important considering 75% of persons infected with HIV in the United States were at or below the poverty level [72].

The most popular platform for CLIA-waived rapid diagnostic tests has proven to be immunochromatography. This is partially due to the simplicity by which high signal intensity and clarity can be achieved as well as financial considerations.

2.2.5 Immunochromatographic Assays

Immunochromatographic assays are available as over-the-counter tests for several conditions, such as pregnancy, drugs of abuse, HIV, and other conditions [46, 47]. The antibody labels used in this test, commonly gold nanoparticles are typically visible with the naked eye. This eliminates the need for expensive equipment required to provide the user with an output [46, 47].

The immunochromatography technique allows for visible detection of an antigen in a sample by the naked eye, eliminating the need for expensive equipment availability to the end-user. An antibody is typically optically labeled with a colored nanoparticle. Oftentimes, the labels of choice are gold nanoparticles of various sizes, typically between 5-50 nm [51, 73-87]. Gold nanoparticles in this size range allow for a much higher specific surface area compared to those of the same optical density in the 100-200 nm range or larger [47]. This allows more analyte-detecting proteins to be immobilized to the surface, increasing the sensitivity of the immunoassay [47]. Compared to larger nanoparticles, there is less variability in the signal brightness with concentration of analyte when using smaller nanoparticles [47]. The small size of the gold nanoparticle label does not interfere with the flow and migration of the labeled antibody through the membrane to the reactive zone [54, 88]. The excellent optical properties of gold

nanoparticles allow for increased sensitivity of the immunochromatographic assays, revealing presence of analyte in the ng/ml range [54, 73, 88]. Pregnancy tests are immunoassays that generally detect the presence of human chorionic gonadotropin (hCG) in urine samples. An independent evaluation of over-the-counter pregnancy tests found sensitivities in the 25-100 mIU/ml, or approximately 2-7 µg/ml [89, 90]. Other immunoassays can show higher sensitivity. Lateral-flow rapid influenza diagnostic tests have shown sensitivity in the ng/ml range.

While expensive equipment is not required and less skill is involved in administering lateral flow immunoassays, issues with sensitivity have become apparent. Rapid influenza diagnostic tests (RIDTs) have been shown to provide sensitivities less than 40-60% in adults [65]. This may lead to the need for confirmatory testing to be carried out, further increasing the cost of the diagnosis and treatment of the patient.

Lateral-flow diagnostic tests are not limited to the healthcare setting. They have been employed in a variety of fields other than healthcare. They have been shown effective in forensics [88, 91], pathogen detection in feed [73, 74, 80, 88, 92-96] and plants [55, 73, 88], as well as for ecological samples such as soil and water [73, 75, 88, 97]. These lateral-flow diagnostic tests can be used at the point-of-care or industry setting as well as for in-home diagnoses.

2.2.6 At-Home Diagnostic Tests

The most popular configuration for these tests is the lateral flow immunoassay (LFIA) tests. Generally these tests have several components: a sample pad to which

specimen is added, a conjugate pad with labeled antibodies specific to the antigen of interest and control antibody or molecule immobilized in the test region, a membrane testing zone with a test antibody specific to the analyte and a control antibody specific to the antibody labeled in the conjugate pad, and a reservoir that provides extra wicking forces and retention of labeled antibody that does not react with the test or control stripes. All these components are attached on a plastic backing. The reservoir pad is made of absorbent material that enhances wicking along the membrane to ensure all possible conjugates reach the reaction zone and reduces background noise. The testing membrane is typically composed of nitrocellulose. The conjugate pad is often a borosilicate glass fiber pad with low-retention characteristics allowing it to release dried gold nanoparticle-labeled antibody to the nitrocellulose membrane. The sample pad is usually an absorbent material, such as cellulose. A schematic of the general LFIA diagnostic tests is shown in Figure 2. The cost of these LFIA diagnostic tests can be high. The OraQuick® In-Home HIV costs $39.99 per test kit. There exists a need to reduce the cost of these in-home tests, to increase availability to patients with minimal resources. This is especially important considering 75% of persons infected with HIV in the United States were at or below the poverty level [72].

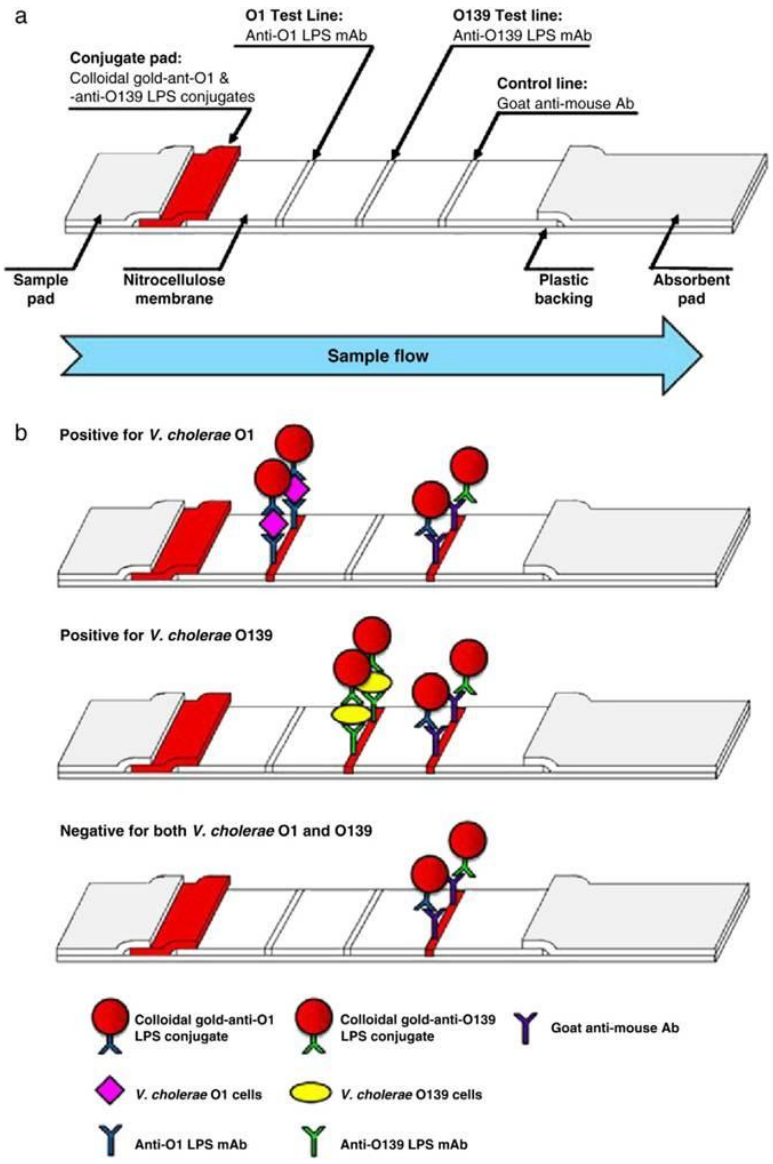

Figure 2. A schematic representative of typical lateral-flow immunoassay devices. Shown here are the components (a) the sample pad, conjugate pad with gold-antibody conjugates, test lines, and control line on the nitrocellulose membrane, and the absorbent pad, all on the plastic backing. Also shown is the procedure and possible results (b) for gold-labeled antibodies recognizing antigens as well as the control line antibody (goat anti-mouse).This schematic was reproduced from a study by Choo Yee Yu et al [79].

Chapter 3
Specific Aims and Significance

3.1 Significance

Currently, immunochromatography principles are utilized in diagnostic tools for clinical laboratory, point-of-care, and in-home testing. The diagnostic tools have proven valuable in decreasing the diagnosis turn-around time for patients when compared to conventional methods, such as viral cell culture [5-7]. In many cases, such as lateral flow immunoassays for diagnosis of influenza, this is largely due to the ability of the tests to be administered at the point-of-care. Other diagnostic tests, such as pregnancy tests, can be purchased over-the-counter for an at home diagnosis. The simplicity of the lateral flow immunoassay platform allows them to be administered with little training and with little chance of error. However, these diagnostic tools do have limitations effecting their efficacy and availability to the full market potential, most notably, cost and sensitivity. Rapid influenza diagnostic tests (RIDTs) have been shown to have sensitivities <40-60% in adults [65]. This sensitivity may be increased by developing a nanofiber-based immunoassay platform. The high specific surface area of nanofiber yarns and different detection antibody immobilization techniques may increase the sensitivity of the diagnostic tests. Another concern for the RIDTs is the availability to the patient. Sample collection and processing does not allow for these tests to be purchased over-the-counter for in-home diagnoses. Decreasing the discomfort and complexity of these tests may

increase the availability of diagnostic testing and quality of healthcare to patients that are unable to make it to a point-of-care diagnostic testing facility. The manufacturability of these diagnostic tests can also be increased. Reducing the components utilized in the manufacturing of these tests can reduce cost and increase the manufacturability. A fiber-based immunoassay system may be incorporated in multiple configurations, which may not necessitate individual housing and packaging of tests.

3.2 Specific Aims

3.2.1 Development of a Fiber-based Immunoassay System

This study aims to incorporate immunoassay technology that is currently used for diagnostic tests into a fiber-based system to: increase the sensitivity, decrease the number of components in manufacturing, thereby reducing cost, and facilitate simpler and more comfortable sample collection to simplify the procedure. Several goals need to be accomplished for successful development, verification, and validation of this system.

3.2.1.1 Preparation of Immunoassay Yarns

Electrospun polymer nanofiber yarns were prepared and characterized, yielding a high specific surface area. The several different compositions of yarn will be examined for feasibility of employment into an immunoassay system. The ability to bind antibodies using a covalent cross-linker will be determined as well as the retention of antibody activity after yarn functionalization. The blocking procedure is also verified to ensure no loss of functionality occurs.

3.2.1.2 Preparation of Colloidal-Gold Labeled Antibodies

Colloidal-gold labeled antibodies will be prepared to detect analyte in solution and provide an optical signal as an output on the surface of the nanofiber yarns. Complete adsorption of protein to the gold nanoparticle surface will be verified via flocculation tests.

3.2.1.3 Fiber-based Immunoassay Performance

After the components to be employed in the immunoassay system have been verified, the viability of their employment will be validated using model antibody-analyte systems. Performance will be assessed by the signal provided for positive and negative analyte samples, based on clarity and intensity.

Chapter 4

Preparation of Nanofiber Yarns

4.1 Introduction

Antibodies have been shown to physically adsorb against many substrates, while retaining their specific activity towards an antigen. Many lateral flow immunoassay membrane preparation techniques employed in industry and academia rely on the electrostatic interactions of the antibodies to the nitrocellulose membranes [75, 76, 80, 98]. Oftentimes, the antibody is dispersed on the nitrocellulose membrane by a jet dispenser in a low-volume state. This prevents antibody spreading by capillary forces along the membrane, leaving sharp and distinct physically adsorbed antibody stripes. This method of antibody immobilization relies on electrostatic interactions. Other materials that are used as the test membrane rely on hydrophobic interactions. The physical adsorption of antibody to a surface can cause the antibody to lose some activity due to orientation of the antibody. It has been shown that 90% of physically adsorbed antibody may be in an orientation that causes complete loss of activity due to steric hindrance of the antigen binding site [53, 99, 100]. Additionally, covalently cross-linked antibody can be immobilized with higher efficiency than physically adsorbed antibody. Thus, to immobilize antibodies to our nanofiber yarn, we will utilize a photo-reactive covalent cross-linker.

Chemical modification of antibodies has been shown to decrease or completely inhibit antibody activity by masking the epitopes for antigen binding. This is especially of concern for monoclonal antibodies, as they are only able to recognize one epitope [29]. Thus, attachment of antibodies to biosensor substrates is often accomplished by physical adsorption. The antibody-substrate hydrophobic interactions can be undefined and lack stability which can cause activity loss and low binding efficiency of the antibody to the substrate [101-106]. Covalent attachment of antibodies to the substrate can define the region of the antibody that is bound to the surface of the biosensor, ensuring activity and availability of the antigen binding region [101-104, 106]. Covalent antibody attachment to a substrate also has higher reproducibility compared to physical adsorption methods [107]. Heterobifunctional photo-reactive cross-linkers have been shown to be effective in immobilizing biomolecules on polymeric substrates while retaining antigen binding availability and activity [101-106]. One moiety of the photo-reactive cross-linker is activated by UV light to react with the substrate, while the other specifically binds the biomolecule of interest to the photo-reactive cross-linker [103, 106]. Common photo-reactive cross-linkers that have been studied are ketyl-reactive or nitrene/carbene-reactive cross-linkers. Diazirine compounds are carbene-reactive photo-reactive cross-linkers [101, 103, 106, 108, 109]. The diazirine moiety is activated by long-wave (330-370 nm) UV irradiation to form a carbene intermediate, which can then insert via addition reactions with carbon-carbon double bonds, reaction with activated carbon-hydrogen or nitrogen-hydrogen bond, oxygen-hydrogen bonds, or sulfur-hydrogen bonds. This allows

the photo-reactive cross-linker to form stable conjugates with the substrate, amino acid side chains or peptide backbones [101, 103, 106, 108, 109]

There are several methods that have been shown to determine antibody activity quantitatively [110], semi-quantitatively [111], and qualitatively [107]. Fluorescent immunohistochemical staining was chosen to verify antibody activity retention after cross-linking the antibody to the nanofiber yarn.

4.2 Materials and Methods

4.2.1 Materials

Electrospun nanofiber yarns were prepared by our collaborators with compositions of poly(vinylidene fluoride)/poly(ethylene oxide) (PVDF/PEO), PVDF, polyacrylonitrile (PAN), cellulose acetate/polyacrylonitrile (CA/PAN), cellulose acetate/poly(methyl methacrylate) (CA/PMMA), and poly(methyl methacrylate/poly(ethylene oxide) (CA/PMMA/PEO). Rabbit anti-bovine IgG, FITC-labeled goat anti-rabbit IgG, bovine anti-mouse IgG, biotinylated bovine anti-mouse IgG, mouse anti-FITC IgG, biotinylated mouse anti-FITC IgG, and goat anti-mouse IgG antibodies were purchased from Sigma-Aldrich Corporation. Streptavidin was purchased from Rockland Immunochemicals, Inc. The photo-reactive sulfo-NHS-LC-diazirine cross-linker was purchased from Thermo Scientific, Incorporated. The fluorescent dyes used for labeling were Alexa Fluor® 350, 488, and 594 were purchased from Life Technologies Corporation (Invitrogen™). Fluorescein Isothiocyanate (FITC) was purchased from Alfa Aesar. Blocking solutions of ethanolamine (Acros Organics), bovine

serum albumin (BSA) and Tween 20 (Acros Organics) were made in 10 mM phosphate buffered saline buffer purchased from Fischer Scientific. The Spectroline® Model XX-15A long wave ultraviolet light lamp (365 nm) was purchased from Spectronics Corporation.

4.2.2 Yarn Preparation

Nanofiber yarns were prepared by the electrospinning method report previously by our collaborators: Chen-Chih Tsai, et al [112]. To determine the porosity of the yarn a tributyl phosphate (TBP) droplet of known volume (V_d) was added to a yarn of lesser volume (V_y), such that $V_d > V_y$. The radius of the yarn (R_y) was measured by optical microscopy (Olympus BX-51) and used to calculate the volume of the yarn (V_y) of a known length (L) with the following equation: $V_y = \pi R_y$L. After complete wetting of the yarn by the TBP droplet, the yarn was placed on a scale (Sartorious, BP-221S) for mass measurement. The low vapor pressure of TBP (0.00012 mm Hg at 25°C) prevents evaporation of the TBP throughout procedure and measurements. The porosity of the yarn was then calculated as $\varepsilon = (m_w - m_d)\ \rho V_y$, where m_w is the mass of the completely wetted yarn, m_d is the mass of the dry yarn, ρ is the density of TBP (0.979 g/cm^3), and V_y is the volume of the yarn. The average porosity of three CA/PMMA/PEO yarns was found to be $\varepsilon = 0.61 \pm 0.04$. The methodology to determine the yarn permeability described in a paper by Callegari, et al was utilized here [113]. The permeability of the yarn was determined to be $k = 8.84 \times 10^{-13}$ m^2. The scaling arguments suggest that the interfiber distance is measured as $d \sim k^{1\ 2} \sim 1\ \mu m$ [114].

4.2.3 Yarn Functionalization

The efficiency of antibody immobilization on various nanofiber yarn compositions is another important parameter to consider when selecting a material for the immunoassay yarn. To this end, antibodies labeled with fluorescent dyes were covalently attached to the fiber surface of the various compositions: PVDF, PVDF/PEO, PAN, CA/PAN, CA/PMMA, and CA/PMMA/PEO yarns.

The antibodies to be immobilized on these nanofiber yarns (goat anti-rabbit IgG and rabbit anti-bovine IgG) were purified from sodium azide by centrifugal filtration. The pure antibodies were then re-suspended in 1X PBS (pH 7.4). The UV-sensitive sulfo-NHS-LC-diazirine cross-linker was dissolved in 1X PBS at a concentration of 1 mg/ml. The goat anti-rabbit IgG and rabbit anti-bovine IgG antibodies were added to separate aliquots of the sulfo-NHS-LC-diazirine solution and incubated with shaking at room temperature for 1 hour to allow for conjugation of the UV-sensitive cross-linker to the antibodies. The antibody-cross-linker conjugates were then purified from excess sulfo-NHS-LC-diazirine by centrifugal filtration and re-suspended in 1X PBS (pH 7.4).

To prevent capillary pressure wicking reactive antibodies towards each other, a 2 µl droplet of 10 mM PBS was added to the center of the CA/PMMA/PEO nanofiber yarn. A 2 µl droplet of goat anti-rabbit IgG was added 1 cm from one end of the yarn and a 2 µl droplet of rabbit anti-bovine IgG was added to 1 cm from the other end of the yarn immediately following the addition of the PBS droplet. A 2 µl droplet of 10 mM PBS was then added to each end of the yarn. Slits were cut in a UV-protective mask to ensure

that narrow and distinct antibody stripes were immobilized on the yarn. The masked CA/PMMA/PEO nanofiber yarn loaded with antibody-cross-linker conjugates was exposed to UV light at 365 nm for 20 minutes. This method was proven effective by immobilizing fluorescently labeling reactive antibodies with Alexa Fluor® 488 and Alexa Fluor® 594, respectively, on a CA/PMMA/PEO nanofiber yarn and imaging with fluorescent microscopy. Independent and distinct antibody stripes would show fluorescence from the Alexa Fluor® 488 dye only at the site of the 488 labeled antibodies, and no 488 fluorescence at the location of the Alexa Fluor® 594 labeled antibody, and vice-versa.

The yarn was then dried by wicking the fluid away simultaneously at each end with a tissue. The yarn was then washed by adding a droplet of PBS to the center of the yarn and wicking the fluid away simultaneously at both ends. The washing of the yarn by wicking from the center to both ends of the yarn simultaneously allows the excess antibody to be removed from the yarn without reacting with the other antibody immobilized on the yarn. The antibody-conjugated CA/PMMA/PEO yarn was then blocked in a 5% (w/v) bovine serum albumin (BSA) solution at 37°C for 3 hours. The optimum yarn blocking solution was determined by blocking the CA/PMMA/PEO nanofiber yarns with 1% Ethanolamine, 1% Ethanolamine with 0.05% Tween 20, 5% (w/v) BSA, and 5% (w/v) BSA with 0.05% Tween 20. These yarns were then coated with platinum and examined by scanning electron microscopy (Hitachi S4800).

4.2.4 Antibody Activity

For the development of an immunoassay system, it is important that the detection biomolecules or antibodies in this case, are capable of recognizing the target analyte, also antibodies for this system. Because chemical modification can potentially mask the binding moieties of antibodies, a system without chemical modification was used to validate antibody-antibody interactions.

The streptavidin-biotin reaction has been shown to have extremely high affinity capable of being applied in biosensor applications [1, 6, 115-117]. From this knowledge, it can be concluded that immobilization of streptavidin on the nanofiber surface followed by subsequent streptavidin-biotin reaction with a biotinylated antibody without losing loading efficiency of antibody on the nanofiber yarn. This reaction may, in fact, increase the loading efficiency of antibody on the nanofiber yarn and increase the sensitivity of the immunoassay system. This system will also eliminate the need for chemical modification of the antibody which could potentially result in loss or complete elimination of antibody activity. In order to confirm activity of the antibody after cross-linking streptavidin to the nanofiber substrate then adding biotinylated antibody to react with the immobilized streptavidin and followed by the addition of antigen to the yarn, immunohistofluorescence staining was performed.

Streptavidin was cross-linked to the yarn with the heterobifunctional photo-reactive sulfo-NHS-LC-diazirine cross-linker using the same method as described previously for antibody attachment to the nanofiber yarn. Streptavidin (1 mg/ml) was

incubated with sulfo-NHS-LC-diazirine cross-linker in 10 mM PBS at room temperature for 1 hour with shaking at room temperature. The streptavidin-cross-linker was then purified from excess cross-linker by membrane centrifugation. Small droplets of streptavidin were then added to the yarn at two different locations, where the test and control antibodies will be attached. A mask was made by cutting slits in aluminum foil to protect the areas of the yarn where streptavidin is not wanted to be immobilized. This mask will allow for the covalent attachment of two sharp and distinct stripes of streptavidin for reaction with biotinylated antibody. Non-covalently attached streptavidin was then washed away from the yarn by wicking PBS buffer along the entire length of the yarn.

Biotinylated bovine anti-mouse IgG and mouse anti-FITC IgG were labeled with Alexa Fluor® 488 and 594, respectively. A 2 µl droplet of PBS was added in the middle of the yarn, between the two streptavidin stripes immediately before the simultaneous addition of the antibody droplets. This was necessary to prevent wicking of the antibodies along the length of the yarn to the other antibody stripe. Had this occurred, the bovine anti-mouse IgG would recognize the mouse anti-FTIC IgG at both locations and fluorescence from both would be evident. After addition of the antibodies to their respective streptavidin stripes, the yarn was incubated for 30 minutes at room temperature to facilitate the streptavidin-biotin reactions. To remove the un-reacted antibody from the yarn, the yarns were washed by wicking of a PBS droplet from the center of the yarn to both ends. This washing method was employed to prevent wicking of the excess antibodies to the other antibody stripe, where the bovine anti-mouse IgG

would recognize and bind to the mouse anti-FITC IgG, resulting in fluorescence from the 488 and 594 dyes at both locations. The yarns were then blocked by immersion in 15 ml of 1% ethanolamine blocking solution and incubated for 3 hours with shaking at 37°C.

Bovine serum albumin (BSA) was labeled with FITC by adding FITC to BSA in 0.1 M sodium bicarbonate buffer and incubating at room temperature with shaking for 2 hours. Excess FITC was purified from the FITC-labeled BSA by membrane centrifugation and re-suspending the FITC-labeled BSA in PBS, and then dialyses against PBS. Mouse anti-FITC was labeled with Alexa Fluor® 350.

4.3 Results and Discussion

4.3.1 Yarn Functionalization

All yarn compositions allowed for antibody immobilization on the nanofiber surface using the photo-reactive cross-linker. The method for covalently immobilizing antibodies to the CA/PMMA/PEO nanofiber yarns and preventing reactive antibodies from interacting with each other was proven effective. Typical results are shown below in Figure 3. Green fluorescence from Alexa Fluor® 488 can be seen only at the bovine anti-mouse stripe, while red fluorescence from Alexa Fluor® 594 can be seen only at the mouse anti-FITC stripe.

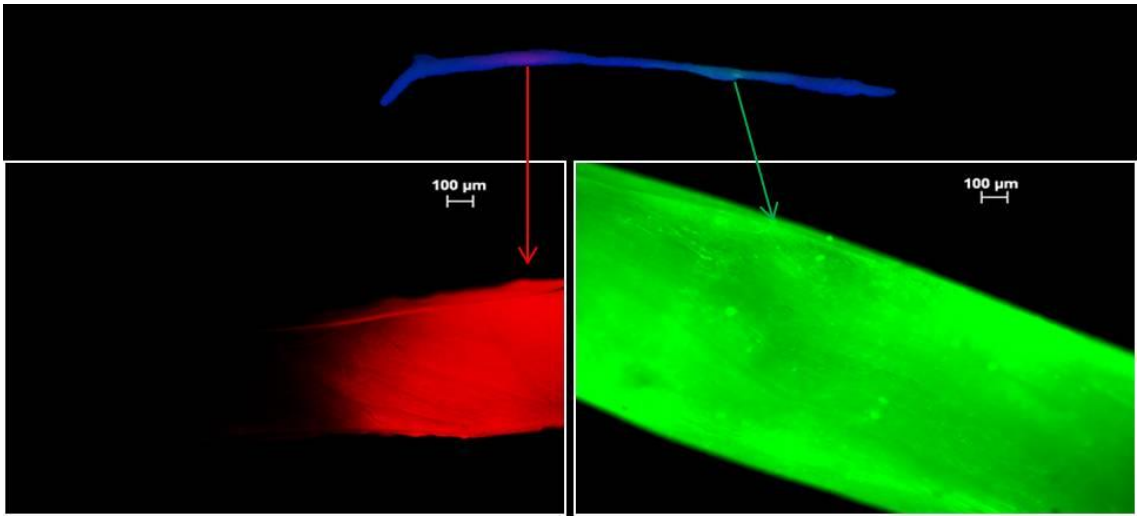

Figure 3. Typical results of antibody immobilization on yarn via sulfo-NHS-LC-diazirine followed by washing and blocking steps. Alexa Fluor® 594 labeled mouse anti-FITC (left) and Alexa Fluor® 488 labeled bovine anti-mouse IgG (right) are shown with fluorescent microscopy (bottom) and as visible by the naked eye after UV excitation (top).

The droplet of buffer in the middle of the yarn prevented capillary forces that would have wicked the antibodies toward one another. Had this happened the antibodies would have reacted and potentially lost reactivity and been unable to recognize analyte in the final immunoassay system. Washing by wicking the droplet away from the center allowed the capillary pressure to wash the antibody from each stripe away from the other stripe, preventing antibody reaction throughout this step as well.

4.3.1.1 Determination of Optimal Blocking Method

The SEM images used for analysis of the different blocking solutions can be seen below in Figure 4. Nanoporous structures can be seen in the 5% BSA with 0.05% Tween 20 and 1% Ethanolamine with 0.05% Tween 20 blocking solutions. Nanoporous structures can also be seen in the CA/PMMA/PEO yarn that has had the PEO washed out

in MilliQ water. Crystal structures can be seen on the surface of the CA/PMMA/PEO nanofibers that have been blocked with ethanolamine blocking solutions.

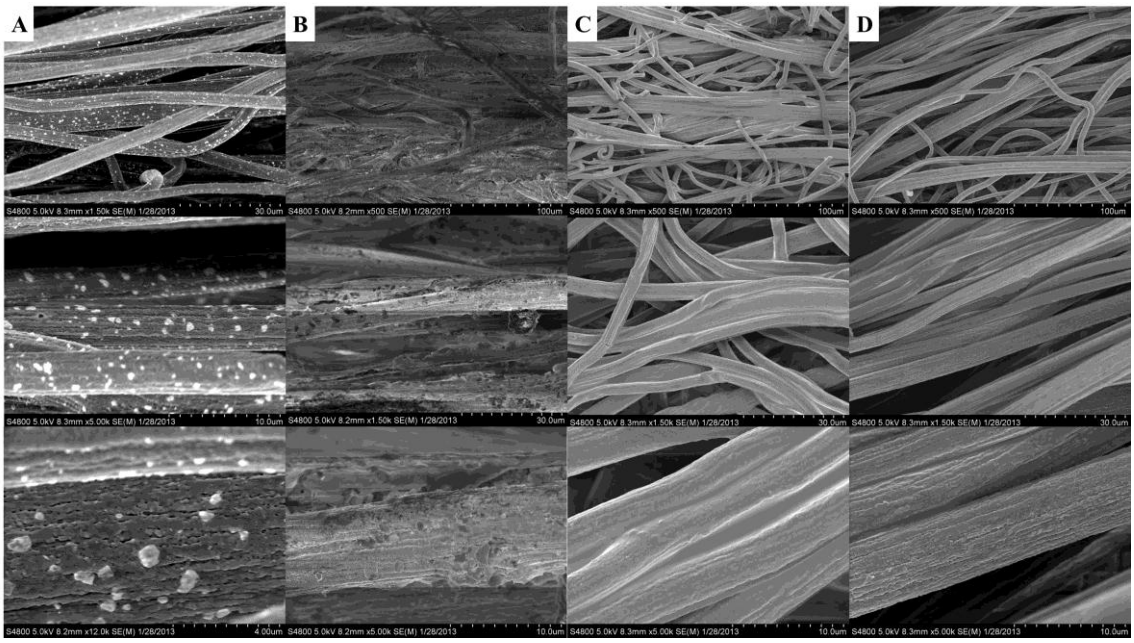

Figure 4. The surface topography of the CA/PMMA/PEO yarns after blocking in 1% Ethanolamine, 1% Ethanolamine with 0.05% Tween 20, 5% BSA, and 5% BSA with 0.05% Tween 20, in order from left to right.

The SEM investigation on the effect different blocking solutions have on the surface topography of the nanofibers was quite interesting. The blocking solution chosen for the remainder of the study was the 5% BSA solution without the presence of Tween 20. The ethanolamine blocking solutions affected the surface topography, and could ultimately have some influence in the wicking properties of the final immunoassay yarn. The blocking solutions that contained Tween 20 also showed changes in surface topography compared to the unmodified yarns. Some nanoporous pitting is evident on the surface of the 1% ethanolamine with 0.05% Tween 20 blocked yarn and on the 5% BSA

with 0.05% Tween 20 blocked yarns, but not on the 1% ethanolamine and 5% BSA blocked yarns. Thus, 5% BSA without any Tween 20 is the best blocking solution to use for this application. It allows the fibers to keep the surface topography of the unmodified CA/PMMA/PEO yarns. This will prevent any decrease in wicking of nanoparticle conjugates in the final immunoassay system due to hindrance by rough surfaces of the yarn or entrapment in holes and pits on the surface of the fibers. Also evident from the SEM images of different CA/PMMA/PEO yarns was that washing the yarns in water overnight resulted in pitting and porous structures in the surface topography of the fibers, due to the washing out of PEO from the yarn structure.

4.3.2 Antibody Activity

There is fluorescent signal apparent at the site of streptavidin immobilization with the photo-reactive cross-linker, shown in Figure 5. After the incubation of streptavidin functionalized yarns with biotinylated bovine anti-mouse IgG and biotinylated mouse anti-FITC IgG antibodies, fluorescent signal was apparent from the Alexa Fluor® 350 and Alexa Fluor® 594 dyes, respectively. Mouse anti-FITC IgG labeled with Alexa Fluor® 594 was then added to the yarn with the streptavidin-biotin-bovine anti-mouse IgG functionalization and a control yarn. Fluorescent signal from the red dye was only visible on the streptavidin-biotin-bovine anti-mouse IgG functionalized yarn. The fluorescent signal ratio of the test yarn to the control yarn was 3.3:1. The yarn functionalized with streptavidin-biotin-mouse anti-FITC and the control yarns were incubated with FITC labeled BSA. After washing of the yarns the functionalized yarn

showed higher fluorescent signal from the FITC label than the control yarn, with a fluorescence ratio of 1.7:1. Immunohistofluorescence images are shown below in Figure 6.

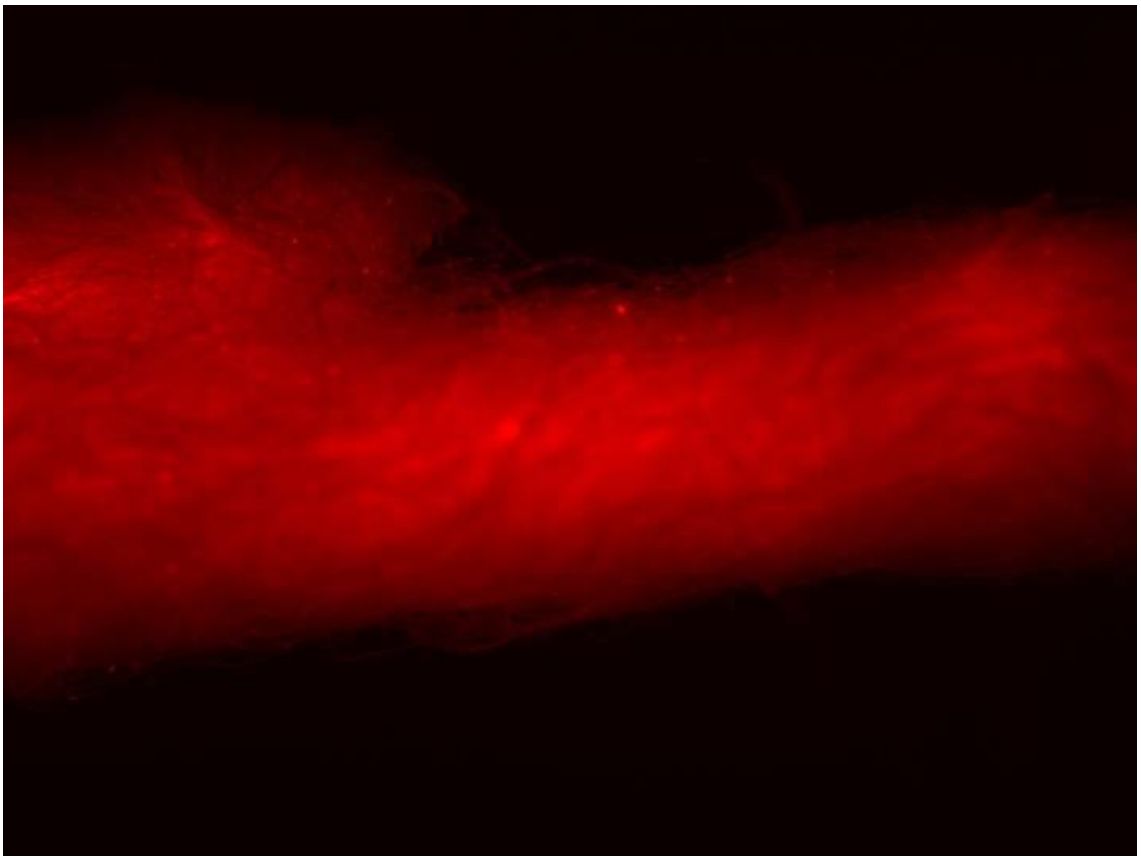

Figure 5. Shown here are typical results seen from immobilization of fluorescently labeled streptavidin to the CA/PMMA/PEO nanofiber yarns by the photo-reactive cross-linker. This streptavidin was labeled by Alexa Fluor® 594 dye.

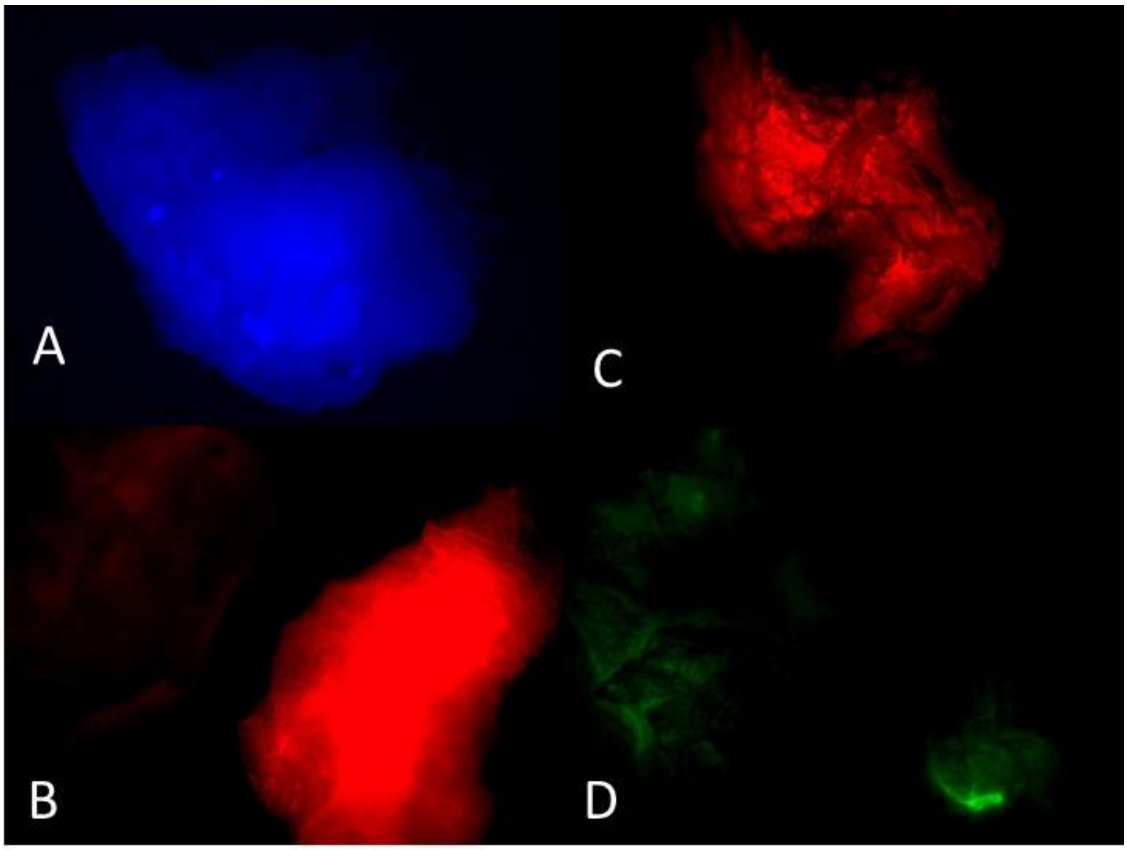

Figure 6. Shown here are results from the immunohistofluorscence study with the streptavidin-biotin system. (A) Biotinylated bovine anti-mouse IgG, labeled with Alexa Fluor® 350, and (C) biotinylated mouse anti-FITC IgG, labeled with Alexa Fluor® 594, functionalized yarns were incubated with mouse-anti-FITC (B), labeled with Alexa Fluor® 594, and FITC labeled BSA (D), respectively. Control yarns are also shown after analyte addition.

The immunohistofluorescence studies showed that the streptavidin-biotin antibody system could be utilized in the development of the immunoassay systems. It is important to note that the streptavidin-biotin-mouse anti-FITC functionalized yarn was smaller than the control yarn, which may initially appear as more fluorescent to the naked eye. The streptavidin-biotin system could potentially be used to increase the sensitivity of the immunoassay system or be used in the case of antibodies that lose activity due to modification by the photo-reactive cross-linker [6].

Chapter 5
Preparation of Gold-labeled Antibody

5.1 Introduction

The synthesis of gold colloid is fairly well known, despite the fact that the mechanism is still up for debate [118]. Turkevich originally proposed the "organizer model" for gold nanoparticle nucleation [119]. Other mechanisms proposed include been the synthesis begins with large particles that shrink with increase reaction time [118, 120], and nanowires smooth to nanoparticles [118, 121] or fragmentation into spherical nanoparticles with citrate adsorption [118, 122]. The nanoparticles synthesized can be tailored to narrow size distributions to fit the needs of the application they will be used in. The most common method is citrate reduction, known as the Turkevich method [119], where citrate serves as the both the reducing agent and the stabilization agent. Trisodium citrate dehydrate is added to a boiling solution of $HAuCl_4$ with stirring. The color of the solution darkens into a deep wine red, which indicates the completed colloid formation [118, 119, 121, 123-126]. Size of the nanoparticles can be altered by modification of the reaction conditions such as the pH, temperature, and the concentration of trisodium citrate and gold [118, 119, 121, 123-126].

Gold has been shown to have an extremely high affinity for protein adsorption [110]. Gold chips are employed in SPR studies as the substrate to which antibodies are bound to determine their binding affinity towards antigens [107, 110]. Gold also has a

very high optical density and has found application in various techniques for labeling proteins in lateral flow immunoassays and labeling of cellular components in electron microscopy [127, 128]. Antibodies have frequently been labeled by gold colloid [110, 123, 129]. The proteins bind to the gold nanoparticles by electrostatic and hydrophobic interactions [129]. Gold colloid will serve as the antibody label used to detect analyte in our final immunoassay system.

5.2 Materials and Methods

5.2.1 Materials

Bovine anti-mouse IgG and goat anti-rabbit IgG were purchased from Sigma-Aldrich Corporation. Different gold nanoparticles were used throughout the development of the immunoassay: 5 nm gold colloid was purchased from British Biocell International and 25 nm Gold Sol purchased from Aurion.

5.2.2 Preparation of Colloidal Gold-Labeled Antibodies

The goat anti-rabbig IgG antibody to be labeled with gold nanoparticles was purified by centrifugal filtration and re-suspended in 5 mM sodium bicarbonate (pH 9.0). Purified goat anti-rabbit IgG was added to stock colloidal gold un-stabilized in water and was incubated with shaking for 30 minutes at 37° C. To further stabilize and block non-specific binding of the antibody-gold nanoparticle conjugates, a 10% solution of BSA was added to bring the conjugates to a final concentration of 1% BSA. The excess protein

was purified from the conjugates by centrifugation at 5000 rcf for 30 minutes. The fluffy pellet was then re-suspended in PBS (pH 7.4) with 1% BSA (w/v).

The stabilizing quantity of goat anti-rabbit antibodies required was determined by a flocculation test performed by a hybrid of flocculation tests performed in industry and reported in literature and manufacturers [79, 123, 130]. Ratios of antibody molecules per gold nanoparticle were calculated, 50,100, 150, 200, 250, and 500 antibody molecules per gold nanoparticle, and added to stock colloidal gold. The solution was vortexed and incubated at room temperature for 2 minutes. A solution of 10% sodium chloride (NaCl) was then added to each mixture ratio of antibody molecules to gold nanoparticles. The absorbance of the colloidal gold labeled antibodies was then measured with a spectrophotometer. Another flocculation test was performed with the only change being the incubation condition the antibodies had with the colloidal gold before the addition of the 10% NaCl solution. The incubation conditions were altered to a 30 minute incubation period at 37°C with shaking after the addition of the antibodies and vortexing to mix thoroughly. The 30 minute flocculation test was only performed for the 200 and 500 antibody molecules per gold nanoparticle ratio. The incubation conditions were altered to allow for sufficient time of antibody adsorption to the gold nanoparticles.

Colloidal gold suspensions are stabilized by the repulsive forces between negatively charged gold and attractive forces. The addition of electrolytes can interfere with the negative charge repulsion forces, leading to aggregation of gold nanoparticles [129]. The presence of enough macromolecules will cause the gold nanoparticles to adsorb to the

macromolecules, instead of each other, thus preventing aggregation. Aggregation of gold nanoparticles will cause a shift in the optical density at specific wavelengths [123, 129]. The ratio that did not cause a color change visible by eye or a significant change in the optical density at 524 nm, the wavelength at which the optical density of stock gold colloid without salt addition was at a maximum, was chosen and used for all antibody-gold nanoparticle conjugate synthesis.

5.3 Results and Discussion

Two different nanoparticle sizes were used throughout the development of the immunoassay system, 5 nm and 25 nm. These sizes were chosen based on the sizes reported in literature being typically between 5-50 nm [51, 73-87]. However, the final size chosen for this immunoassay system was the 25 nm gold nanoparticles, purchased from Aurion because of their ease of use. Nanoparticles were un-stabilized in water as a stock solution. This allowed for elimination of the centrifugation step to remove the stabilizing agents prior to adsorption of antibody. Lower centrifugation speeds could be used for shorter time periods to purify the nanoparticle conjugates from the excess unbound antibody. Paramount among the concerns for choosing a nanoparticle size is the optical signal provided from the nanoparticles in the final immunoassay system. Fewer nanoparticles of the 25 nm size (3.3×10^{11} nanoparticles/ml) result in the same optical density, compared to a larger number (5×10^{13} nanoparticles/ml) of the 5 nm gold nanoparticles, according to each manufacturer's lot specifications. Approximately 150X fewer 25 nm gold nanoparticles could be immobilized at the test and control stripes

compared to the 5 nm gold nanoparticles, with the same visibility. This leads to a potential for increasing the sensitivity of the final system by a factor of 150, approximately.

Stability of the nanoparticle suspensions was checked by dynamic light scattering. The colloid had a monodisperse combined effective diameter of 34.5 nm, with a mean of 35.7 ± 1.7 nm. The stability of the nanoparticle-antibody conjugates was also evaluated with a flocculation test and by optical detection of color change. The results from the flocculation tests are shown below in Figure 7 and Figure 8. The antibody-nanoparticle ratio chosen for conjugate synthesis was 500 antibody molecules per gold nanoparticle with the 30 minute incubation at 37°C conditions. At these conditions, no aggregation of the nanoparticles occurred, as can be observed by no color change detectable by the naked eye and no change in absorbance at 524 nm. The reference solution was the gold colloid solution diluted according to the addition of the proteins and salts for the antibody conjugation test solutions for flocculation. The optical density of the reference solution was maximized at 524 nanometers, with an average optical density of 0.41367. The optical density of the 500 antibody molecules per gold nanoparticle solution was 0.41533 as compared to the decrease in optical density of 0.348 for the 200 antibody molecules per gold nanoparticle ratio. The absorption spectrum of the flocculation tests performed with the 2 minute and 30 minute incubation conditions are shown below in Figure 7 and Figure 8, respectively.

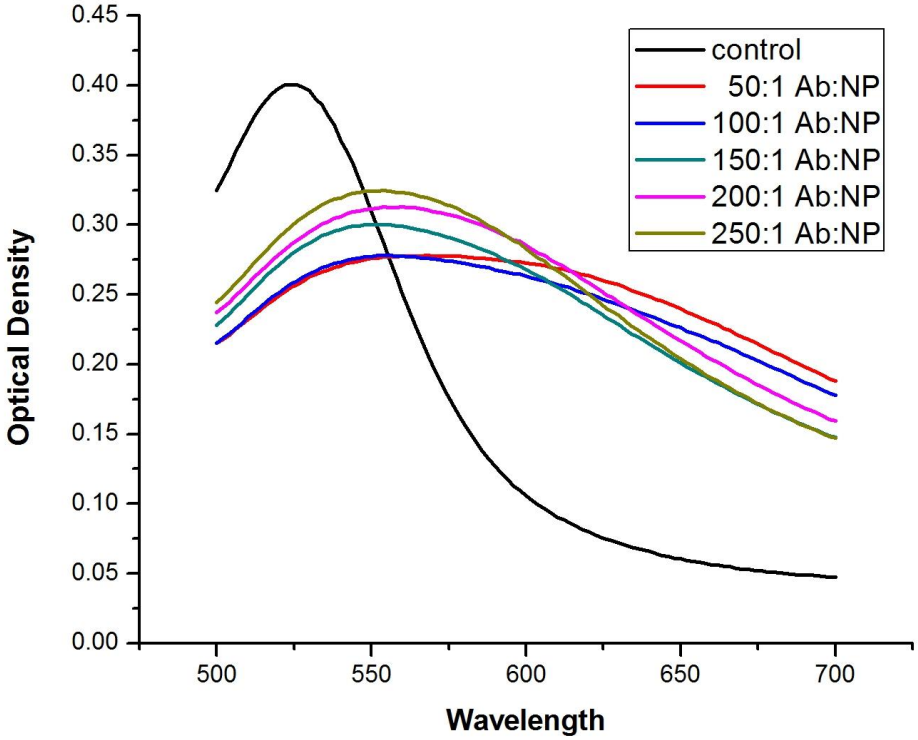

Figure 7.The absorption spectrum of gold colloid solutions after the 2 minute flocculation test. The control used had ultrapure water added to dilute the sample according to the dilution resulting from the addition of the antibodies and 10% NaCl added for the test samples. Antibody was adding according to 50, 100, 150, 200, and 250 antibody molecules per gold nanoparticle ratio, vortexed and incubated for 2 minutes before the addition of 10% NaCl.

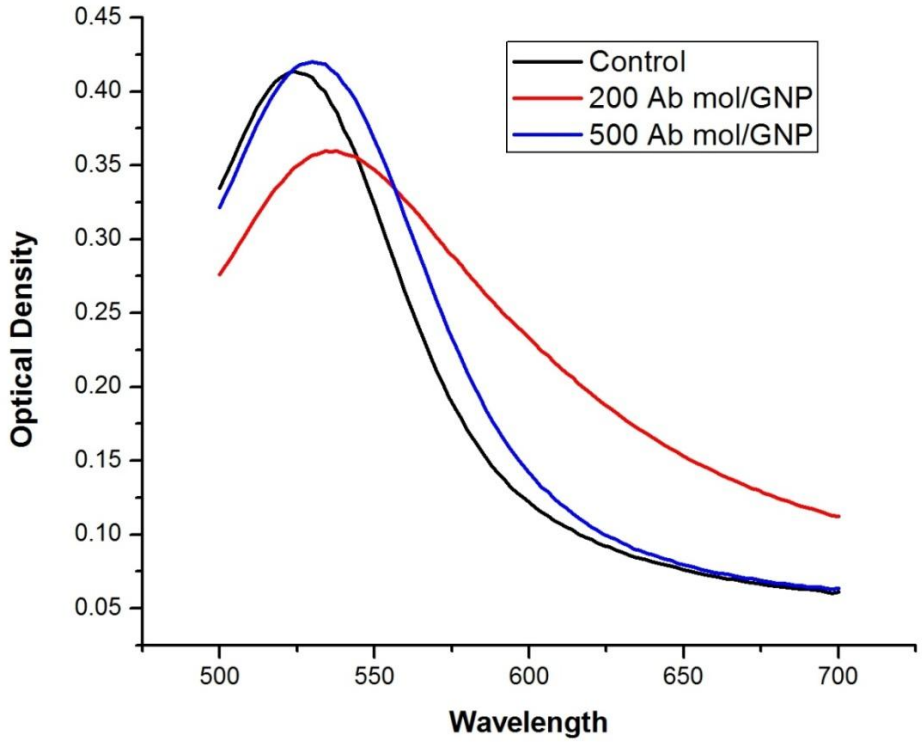

Figure 8.The absorption spectrum of gold colloid solutions after the 30 minute flocculation test. The control was diluted with ultrapure water according to the dilution resulting from the addition of the antibodies and 10% NaCl added for the test samples. Antibody was added according to a 200 and 500 antibody molecule per gold nanoparticle (GNP) ratio, vortexed and incubated for 30 minutes at 37°C for 30 minutes before the addition of 10% NaCl.

Chapter 6

Development of Immunoassay System

6.1 Introduction

Currently, lateral flow immunoassays (LFIAs) are composed of multiple components. Generally, these components include a sample pad, a conjugate pad, a reactive zone membrane, and a reservoir pad. All these components are usually attached to a plastic backing [8, 10, 12, 51, 54, 77, 79, 80, 88-91, 95, 96]. These components limit the configuration in which immunoassays can be employed. This can lead to an increased cost and complexity of manufacturing, and limit the final product configurations of the lateral flow immunoassays. In some cases, additional components, such as swabs, reactants, and buffers, are also needed and used in the process of analyzing a sample for the presence of an analyte. These additional components also lead to additional costs and can increase the complexity of the immunoassay procedure. The increased complexity of the procedure can disqualify some immunoassays from being used for over-the-counter, in-home tests. Limiting the number of components in an immunoassay system can streamline production time and costs, while limiting the number of steps involved in and simplifying the procedure and can make immunoassay detection of conditions available to end-users of varied skill and knowledge levels, allowing for in-home patient use.

While some lateral flow immunoassays can provide excellent sensitivity for a particular application, others have sensitivities that may be insufficient for some samples.

Of particular interest for this paper are immunoassays used to diagnose pathogens or illnesses in patients. Somewhat invasive procedures may be required to retrieve a sample with sufficient analyte concentration by immunoassays with low sensitivities. For instance, commonly used CLIA-waived LFIA tests for influenza require the sample to be collected from nasopharyngeal swabs. Other samples can be used, such as nasal washes and aspirates, but nasopharyngeal swabs are preferred due to the prevalence of antibody and antigen available from nasopharyngeal epithelial cells [11, 61-64]. However, collecting these specimens can be quite uncomfortable and may not be performed by a patient, themselves. If the sensitivity of immunoassays can be increased, there is potential for their deployment to aid in the diagnosis of new conditions with lower concentration analyte or analysis of samples with less concentrated analyte acquired through less invasive and uncomfortable procedures.

One limiting factor for the sensitivity of an immunoassay is the amount of antibody or antigen that can be immobilized on the membrane reactive zone. Due to their high specific surface area, nanofiber yarns can increase the amount of detection molecules attached to the surface that are able to react with analyte. The unique properties of nanofiber yarns have found them to be employed in many different fields including: scaffolds for tissue engineering [131], filtration [132, 133], probes for minute liquid volumes [112], and colorimetric biosensors [134].

Yarns have several other advantages for employment in biosensor applications. The nanofiber yarn-based immunoassay can be employed in multiple final device

configurations. The flexibility of the fibers will allow them to be employed in fabrics such as panty-liners and facial tissues. Surface modification can be readily accomplished [134, 135]. Yarn structures can be oriented to have anisotropic flow properties and have the potential to transport large volumes of fluids [135-137]. The inherent directional flow characteristics of nanofiber yarns will allow the immunoassay yarn to have uniaxial flow of sample fluid. This would also allow the nanofiber yarn immunoassay to be included in facial tissue products, as the analyte will be driven along the longitudinal axis of the nanofiber yarn rather than out to the surrounding tissue.

6.2 Materials and Methods

6.2.1 Materials

The CA/PMMA/PEO yarns were utilized in the further development of the complete immunoassay system. The 25 nm Gold Sol purchased from Aurion was used to label the detection antibodies. The antibody pair chosen for the gold nanoparticles and test and control lines chosen was the FITC-labeled goat anti-rabbit IgG and the rabbit anti-bovine IgG purchased from Sigma-Aldrich Corporation. Borosilicate glass fiber conjugate pads were purchased from EMD Millipore Corporation. Phosphate buffered saline was used at a concentration of 10 mM. Tween 20 (Acros Organics) was added to the concentrated noted in some buffers.

6.2.2 Nanoparticle-Antibody-Analyte Complex Droplet System

Immunoassay yarns and colloidal gold-labeled antibodies were prepared as described previously. The rabbit anti-bovine IgG analyte was added to the colloidal gold-labeled goat anti-rabbit IgG, vortexed, and incubated at 37°C for 30 minutes. The end of the immunoassay yarn was dipped in the resulting droplet of gold nanoparticle-goat anti-rabbit IgG-rabbit anti-bovine IgG complex. Each end of the yarn was dipped in the droplet to ensure the nanoparticle conjugates reached both the test and control lines. The end opposite the nanoparticle droplet was clamped vertically between highly absorbent tissues acting as a reservoir to provide extra wicking forces. Buffer droplets were also applied to each end of the yarn after the nanoparticle conjugate droplets to further push the nanoparticle conjugates along the yarn. A positive result will have two regions of red coloration, at the test and control antibody stripes approximately 25% of the yarn length from each end.

6.2.3 Analyte Yarn System

The goat anti-rabbit IgG and the rabbit anti-bovine IgG immobilized during the preparation of the immunoassay yarn will serve as the test and control stripes for the immunoassay, respectively. Accumulation of antibody-gold nanoparticle conjugates at the test and control stripes will result in a positive test. Accumulation of antibody-gold nanoparticle conjugates at the control line will result in a negative test. Accumulation of the antibody-gold nanoparticle conjugates at the test stripe only will result in an invalid test.

Rabbit anti-bovine IgG was used as a model analyte for our system. A negative control immunoassay was also performed using goat anti-mouse IgG analyte at a concentration of 1 mg/ml. The analyte was added to soak the entire immunoassay yarn for 30 minutes at room temperature. The analyte was then dried by wicking the liquid to a tissue. A 10 µl droplet of PBS with 0.05% Tween 20 was added to the yarn and wicked from the immunoassay yarn to a tissue. This procedure was repeated 15 times to ensure all analyte was washed from the immunoassay yarn and the yarn was dried. A 5 µl droplet of antibody-gold nanoparticle conjugates was added to the immunoassay yarn and allowed to incubate at room temperature. Excess antibody-gold nanoparticle conjugates were wicked away before the yarn dried to prevent non-specific adsorption to the yarn. This procedure was repeated until bright red stripes were visible at the test and/or control lines of the immunoassay yarn.

6.2.4 One-step system

Lateral-flow immunoassays contain a conjugate pad component that houses colloidal gold labeled antibodies in a dehydrated state. Upon addition of sample fluid to the sample pad, fluid migrates to the conjugate pad and re-suspends the colloidal gold-labeled antibodies for migration to and reaction at the reactive site on the nitrocellulose membrane. The housing of these dehydrated nanoparticles allows for use of the system as a one-step diagnostic tool that is much simpler than the analyte yarn system. A one-step system decreases the chance of end-user error that could occur from performing several steps with specific incubation times. In order to implement our fibers into a one-step

diagnostic tool, the gold nanoparticle-labeled antibodies will need to be loaded in a dehydrated state to the immunoassay system

6.2.4.1 Dehydrated Nanoparticle Conjugates on Yarn

Several published articles have reported slightly varying nanoparticle-conjugate dehydration procedures. Components of the buffer used for dehydration generally include sucrose and Tween 20 in a buffer solution. The composition of the dehydration buffer varies slightly [72-74]. A hybrid of these procedures will be used to dehydrate the gold nanoparticles directly to the nanoparticle yarn to retain antibody activity and wickability of the nanoparticles along the immunoassay yarn to the reactive zones for test and control antibodies.

Goat anti-rabbit IgG antibody was labeled with 25 nm colloidal gold by physical adsorption as reported above. The nanoparticle-antibody conjugates were then centrifuged to a soft pellet at 5000 rcf for 30 minutes. The supernatant was removed and the nanoparticle conjugates were re-suspended in PBS with 1% BSA, 1% Tween 20, and 5% sucrose. The nanoparticle conjugates were added to the yarn in very small and concentrated droplets to prevent the wicking of the conjugates along the length of the yarn. The length of the dehydrated gold conjugate region can be described by the equation: $L = V/(\varepsilon\pi R^2)$, where V is the volume of the droplet added to the yarn, ε is the porosity of the yarn, and R^2 is the radius of the yarn. In-between droplet addition, the yarn was dried at 37°C. After complete addition of all gold nanoparticle-labeled antibodies, the yarn was desiccated overnight. To re-suspend the gold nanoparticle-

labeled antibodies droplets of 10 mM PBS buffer and PBS buffer with 0.05% Tween 20 were added to the exact location of the conjugate dehydration. Success in utilizing gold conjugates dried directly on nanofiber yarns will result from re-suspension and migration of the conjugates along the length of the yarn after the drying process, as shown by red coloration of the entire yarn.

A conjugate adsorption experiment was performed to quantify the amount of conjugates irreversibly adsorbed to the nanofiber yarns. A CA/PMMA/PEO film was used to model the surface of the nanofiber yarns. The surface area of the films was measured by Ryan Freed using an interferometer in Dr. Melinda Harman's lab. The lateral surface area of the 12 measured samples, or planar window of measurement, was 4.04± 0.01 mm^2 on average. This accounts for approximately 5% of the total surface area of the film sample. The samples were taken in a 3 sample by 4 sample grid to accommodate for the large scale topographic features relative to the resolution of the interferometer. Large features were able to be included in this grid so that additional error was not incurred by taking surface area measurements where all or most samples could possibly have the same apparent structure, for instance all on the surface of a large spherical bump or all in the valleys between bumps. The average surface area was used to extrapolate the surface area during the conjugate adsorption experiment.

Goat anti-rabbit IgG labeled by FITC was then used to study the protein adsorption to the surface of the CA/PMMA/PEO films. The antibody was diluted to concentrations of 10, 5, 2.5, 1, 0.5, 0.25, 0.1, and 0 μg/ml in 10 mM PBS from a stock

solution of 1 mg/ml antibody. The fluorescence intensity each of these antibody concentrations was measured in triplicate. A polymer film with a lateral surface area of 18 mm^2, corresponding to a surface area of approximately 41.5 mm^2, was then incubated with each sample in a 96 well plate for 1 hour at room temperature with shaking. After the incubation, the polymer films were removed from the antibody solutions and the fluorescence intensity of the antibody solutions was measured again.

The standard curve was obtained by the fluorescence measurements achieved prior to antibody adsorption to the films. Using the standard curve, the protein concentration remaining after adsorption was calculated by the equation, $FI = 8925[P] - 1042.1$, where FI is the measured fluorescence intensity and [P] is the protein concentration remaining in the solution after adsorption. The antibody mass adsorbed to the protein surface was then calculated and divided by the surface area to determine the concentration of antibody adsorbed to the surface of each film. This was then used to develop the Langmuir model of protein adsorption. The adsorption isotherm was developed by plotting the adsorbed protein concentration against the initial protein concentration. Next, the equation: $1\ \ \nu = (1\ \ K)(1\ \ [P_{eq}]) + 1$, was plotted to determine the affinity constant for antibody adsorption. The fraction of protein adsorbed to the film, ν, in comparison with the maximum amount of protein adsorbed was then calculated and the inverse, ν^{-1}, was plotted against the inverse of the equilibrium protein concentration, $[P_{eq}]^{-1}$, as determined by fluorescence intensity. The slope of the linear fit of this line results in the value inverse affinity constant, K^{-1}, from which the affinity constant, K, can

be determined and plugged into the equation: $\Delta G = -RTln(K)$ to determine the Gibb's free energy of adsorption.

6.2.4.2 Conjugate Pad Preparation

Borosilicate glass fiber conjugate pads were purchased from EMD Millipore. Goat anti-rabbit IgG was labeled with gold nanoparticles by the same method as described above. These gold-labeled antibodies were added to the glass fiber conjugate pads by a combination of several methods found in literature [77-79]. The fluffy pellet, however, was re-suspended in PBS with 1% BSA, 1% sucrose, and 0.05% Tween 20 at a 10-fold higher concentration than the stock concentration. This concentration was chosen to reduce the time required to add the gold nanoparticle-antibody conjugates to the conjugate pads. The concentrated gold conjugate solution was added to the conjugate pads. The conjugate pad was dried at 37 °C for 5 minutes after the addition of each droplet. After nanoparticles were loaded onto the conjugate pads they were dried overnight in a desiccator. These conjugate pads were used in the following immunoassay procedures.

Different thicknesses of conjugate pads were used for different immunoassay systems. For the contact conjugate pad immunoassay, a 1 mm thick conjugate pad was used. However to enable twisting of the conjugate pad into the immunoassay yarn structure, much thinner sections of the conjugate pad were required. The typical diameter of the immunoassay yarns is approximately 500 µm. The standard borosilicate glass fiber pads with a 1 mm thickness were mounted on a paraffin block. For our application, the

conjugate pads could not be embedded in the paraffin block, as it may impede migration of the gold nanoparticle conjugates out of the conjugate pad or affect the dehydration of the gold nanoparticle conjugates in the pad. To avoid this, a paraffin block was prepared in a standard way with no conjugate pad. The very top of the paraffin block was then heated to barely melt the surface by pressing a hot, flat metal stamp against the surface. The conjugate pad was then pressed gently against the melted surface and cooled. A microtome (Leica RM 2255) was used to cut 50 µm and 100 µm longitudinal sections from the standard borosilicate glass fiber pads, ensuring that only sections from near the front face, opposite the face attached to the paraffin block, were kept for nanoparticle conjugate loading.

6.2.4.3 Conjugate Pad Contact Immunoassay

An immunoassay yarn was prepared with a goat anti-rabbit IgG test stripe and rabbit anti-bovine IgG control stripe. The borosilicate glass fiber pad was loaded with gold nanoparticle labeled goat anti-rabbit IgG and dried as described above. The conjugate pad was then soaked with rabbit anti-bovine IgG (2.3 mg/ml) in PBS as an analyte solution. The analyte soaked conjugate pad was pressed against the middle of the immunoassay yarn between the test and control stripes. The analyte solution re-suspended the gold nanoparticle conjugates and allowed the yarn to wick the re-suspended gold nanoparticle-antibody-analyte conjugate to be transferred to the yarn and wicked to the end of the yarn by capillary action.

6.2.4.4 Conjugate Pad Incorporated Immunoassay Yarn

Gold nanoparticle-labeled goat anti-rabbit IgG was loaded onto the low retention glass fiber conjugate pads and dried as described previously. The CA/PMMA/PEO nanofibers were twisted around the conjugate pads to form a yarn with the conjugate pad located inside the yarn at the approximate mid-point in length. Goat anti-rabbit IgG and rabbit anti-bovine IgG test and control lines, respectively, were then immobilized, using the UV-sensitive sulfo-NHS-LC-diazirine cross-linker, approximately 1 cm from the either end of the conjugate pad. Very small, 10x concentrated antibody droplets activated with the cross-linker were added at the test and control stripe locations. The small volume droplets were required to prevent the antibody solution from wetting the conjugate pad, thereby releasing the nanoparticle conjugates to the immunoassay yarn. The antibody-immobilized yarn was then blocked with a 5% BSA solution. To prevent the conjugate pad from being wetted by the blocking solution, the conjugate pad was clamped between clean delicate task tissues on each side. Each end of the immunoassay yarn was dipped in a 50 µl droplet of the 5% BSA blocking solution. The capillary pressure of the immunoassay yarn allowed the blocking solution droplet to be wicked to just before the conjugate pad location, where excess was absorbed by the delicate task wipe. After the blocking solution reached its desired height, the blocking reaction was incubated at room temperature for 1 hour. A schematic of the conjugate pad incorporated immunoassay yarn system is shown below in Figure 9.

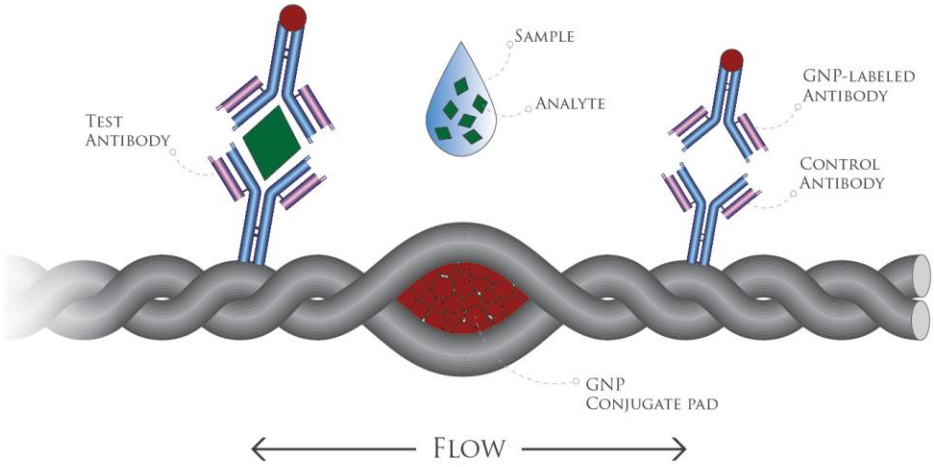

Figure 9.Schematic of the conjugate pad incorporated immunoassay yarn system. Shown here is the conjugate pad twisted in between CA/PMMA/PEO fibers. The test antibody (goat anti-rabbit IgG) and the control antibody (rabbit anti-bovine IgG) are immobilized on the surface of the yarn. The gold conjugates are gold-labeled goat anti-rabbit IgG to detect the rabbit anti-bovine IgG analyte in the sample. As the sample droplet is added the fluid is wicked along the length of the yarn as indicated by the flow direction arrows.

6.2.4.5 Three Yarn System

After consideration of each of the previous systems, another system was developed to provide more confirmatory testing. This system involves inclusion of three yarns: a test yarn which will detect the presence of an analyte in a sample, a positive control yarn which will detect the gold-labeled antibodies, and a negative control sample which will not detect the gold-labeled antibodies or the analyte in question. Antibody immobilization was performed as previously described with the sulfo-NHS-LC-diazirine cross-linker. However, in this instance entire yarns were coated with each antibody without the need for the mask. The test yarn was functionalized with goat anti-rabbit IgG antibody. The positive control yarn was functionalized with rabbit anti-bovine IgG. The negative control yarn was immobilized with goat anti-mouse IgG. After the blocking step was performed the yarns were thoroughly washed by wicking 10 mM PBS as previously described. The test analyte (rabbit anti-bovine IgG) was added to each yarn at a concentration of 100 µg/ml and incubated at room temperature for 30 minutes without drying. The yarns were then washed by wicking 10 mM PBS 10 times. Gold-labeled goat anti-rabbit IgG was then added to each yarn to completely soak the yarn and incubated for 20 minutes at room temperature without drying. The unbound gold-labeled antibodies were then washed away by wicking with 10 volumes of 10 mM PBS.

6.3 Results and Discussion

6.3.4 Nanoparticle-Antibody-Analyte Complex Droplet System

The yarn was not completely wetted by dipping the end of the nanoparticle droplet at one end. After dipping both ends of the yarn, the location of both the test and control lines were wetted and red coloration was apparent. Some red coloration was apparent at the test and control antibody stripe locations, approximately 25% of the yarn length from each end. Red coloration was also apparent at the end of the yarns. Background red coloration was also visible.

Figure 10. Results of the nanoparticle-antibody-analyte complex addition immunoassay. after dipping both ends in nanoparticle droplet and buffer solution. Specific accumulation at the antibody stripes can be seen at the test and control lines approximately 25% of the yarn length from each end. Non-specific accumulation also occurred at the ends of the immunoassay yarn.

The procedure was fairly complex and difficult. Judgment calls had to be made to switch the immunoassay yarn ends in the nanoparticle droplet. The length of the procedure required to see adequate results was also longer than 30 minutes, due to the need to repeatedly add buffer droplets to the end of the yarn to push the nanoparticles to the antibody stripes for optimal signal.

The red coloration apparent at the test and control lines indicates specific nanoparticle-antibody-analyte complex accumulation. The red coloration apparent at the

ends of the yarn indicates non-specific complex accumulation. Because of the significant amount of background signal from the gold complexes, the accumulation at the test and control stripes may be difficult for the end-user to interpret. The nanoparticle accumulation also does not occur in a very sharp and distinct line, as was expected.

These results provide an important proof-of-concept that this immunoassay system does have potential. However, the results are not very clear without room for misinterpretation. The procedure is also rather complex and subjective. Confirmation of specific nanoparticle-antigen-analyte accumulation is also needed. To improve the yarns for application into the immunoassay, fine tuning of the yarn processing, materials and conditions needed to be performed, validating each step in the preparation: the immunoassay yarn recognition and binding of analyte at the test antibody stripe and binding of the nanoparticle-antibody conjugates to the control antibody stripe and the analyte bound to the test antibody stripe, thus a new immunoassay system was introduced.

6.3.5 Analyte Yarn System

Red coloration can be seen at the location of the test and control antibody stripes on the immunoassay yarn with rabbit anti-bovine positive analyte due to antibody-gold nanoparticle accumulation. This yields a positive test for our analyte. Red coloration is visible at only the control stripe location for the immunoassay conducted with the negative control (goat anti-mouse IgG) analyte. Results are shown below in Figure 11.

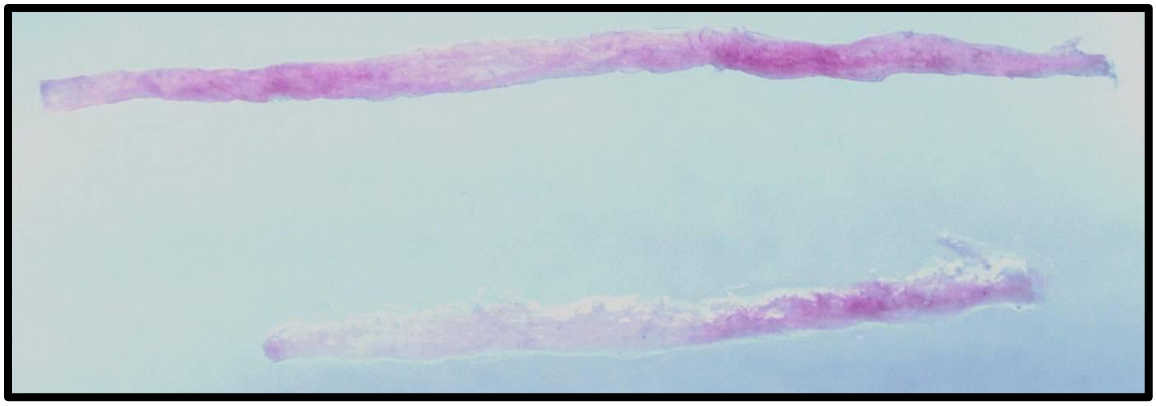

Figure 11. Immunoassay nanofiber yarns with analyte positive sample (top) and analyte negative sample (bottom). Two stripes of gold nanoparticle-antibody conjugate accumulation can be seen in the positive analyte yarn and only one stripe of gold nanoparticle-antibody conjugate accumulation can be seen on the negative control analyte yarn.

This system was performed to verify activity and efficacy of each individual component of the immunoassay system. The covalent antibody attachment has previously been confirmed by fluorescent microscopy; however, the chemical modification by the photo-reactive cross-linker may inhibit the antibodies' recognition of antigens. This system also confirms that the colloidal gold-labeled antibodies are able to recognize the control (rabbit anti-bovine IgG) antibody immobilized on the yarn, as well as the analyte (rabbit anti-bovine IgG) bound to the test antibody (goat anti-rabbit IgG) covalently immobilized to the yarn.

Laboratories currently use multi-step systems to detect the presence of a pathogen, such as PCR and ELISA. These systems may require expensive equipment to obtain good results. The point-of-care system proposed here is procedurally similar to the ELISA technique and requires some technical knowledge or expertise. Those working in a clinical laboratory setting or in hospitals and doctors office that would perform this assay,

such as doctors, nurses, and technicians, should possess the knowledge required to perform and interpret the results of this assay with minimal training. One key advantage of this system is that no expensive equipment is required to read the signal obtained from the assay, unlike the PCR, ELISA and immunofluorescence techniques currently used in clinical laboratories. This dramatically reduces cost and labor time for clinical laboratories and also allows this system to be utilized at the point-of-care.

It was evident by the test and control assays shown in Figure 11 that results can be clearly seen using this technique with little chance of misinterpretation for competent end-users. The procedure is also fairly simple, for clinical laboratory technicians and specially trained nurses or doctors to operate at the point-of-care. The sample is added to the immunoassay yarn and incubated for the antibody recognition reaction to take place and excess is then wicked away. Then, gold nanoparticle conjugates are added to the yarn to recognize the antibodies on the stripes, and the excess is wicked away. Clear results were obtained, but the procedure may be too complex for patients with no technical skill or knowledge to perform the assay as an in-home diagnostic tool. To further simplify the procedure, a one-step methodology was needed.

6.3.6 Dehydrated Nanoparticle Conjugates on Yarn

Nanoparticle conjugates taken from a reagent that needed to be added in a liquid state by trained technicians and were instead added to the immunoassay yarn directly in a dehydrated state. This allows for an immunoassay that only required sample to be added to the nanoparticle conjugate site. Dark red, nearly black coloration was seen at the center

of the yarn after the nanoparticle dehydration procedure. However, the nanoparticle conjugates did not wick along the length of the yarn upon addition of a buffer solution. As a result, this immunoassay system is incapable of detecting antigens present in a sample for analysis. This led to the further investigation into the current LFIA technologies and incorporation of other components as well as the discovery of a promising new potential application for a point-of-care diagnostic tool: the introduction of the borosilicate glass fiber conjugate pad into the immunoassay system.

The conjugate adsorption was then quantified. Measurements of the surface area taken by the interferometer revealed, on average, that the actual surface area/lateral surface area ratio was 2.31± 0.08. Three representative images of the surface area measurements obtained from the interferometer is shown below in Figure 12.

The adsorption isotherm developed during the fluorescently labeled protein adsorption study is shown below in Figure 13. The concentration of adsorbed protein was calculated from the fluorescence intensity using the standard curve, resulting in the equation: $FI = 8925[P] - 1042.1$, where FI is the fluorescence intensity and P is the protein concentration. The fluorescence intensity from the solutions adsorbed to the films was then measured in triplicate and each set of values was plugged into the above equation to find the concentration of antibodies remaining in the solution after the adsorption. This was then used to determine the concentration adsorbed to the surface of the films, [Γ], by dividing the mass of protein adsorbed by the surface area of each film. The adsorption isotherm was plotted as the concentration of antibody adsorbed to the

surface of the films, Γ (μg/cm^2), over the initial protein concentration in solution, [P_0]. The fraction of the antibody concentrations adsorbed to the films, ν, for each equilibrium protein concentration was then calculated assuming the maximum possible antibody concentration was equal to the maximum observed antibody adsorption, [Γ/Γ_{max}]. The inverse of the fraction of antibody adsorbed, ν^{-1}, was then plotted against the inverse of the equilibrium protein concentration, $[P_{eq}]^{-1}$, to determine the inverse of the affinity constant of antibody adsorption, K^{-1}, by finding the slope of the linear fit. The equation: $1\ \ \nu = (1\ \ K)(1\ \ [P_{eq}]) + 1$, is plotted below in Figure 14, such that $\nu \equiv \Gamma/\Gamma_{max}$ which is the fraction of protein adsorbed to the film, K is the affinity constant of antibody adsorption, and [P_{eq}] is the equilibrium protein concentration. The affinity constant, K, was determined to be (3± 0.4) x 10^7, with a linear fit R^2 value for this determination being 0.78. This K value seems appropriate as various protein affinities reported for Nylon-based membranes range from 1 x 10^4 to 2.5 x 10^7 [138]. This linear fitting may be due to the lowest concentration point, where the sensitivity of the instrument may have not been adequate. The affinity constant was then plugged into the equation: $\Delta G = -RTln(K)$, where ΔG is the Gibb's free energy of adsorption, R = 8.314 $J\ \ (mole \cdot K)$, T is the temperature which was 298K, and K is the affinity constant. The results are shown below in Figure 14. The ΔG for goat anti-rabbit IgG adsorption to the CA/PMMA/PEO film was determined to be approximately ΔG= -43 ± 0.3 kJ/mole. The results of the antibody adsorption experiment are summarized in Table 2.The Gibb's free energy of antibody adsorption to the films indicates that the antibodies will adsorb to the CA/PMMA/PEO yarns and may cause the gold-labeled antibodies to stick to the yarn

when applied directly and dehydrated, thereby preventing migration along the nanofiber yarns after addition of aqueous analyte solution. This protein adsorption model is not precise; however it does reveal the expected trend. This model is commonly employed to study the adsorption of protein to surfaces. Assumptions made here are that the maximum protein concentration able to adsorb to the film was that of Γ_{max} such that the film was saturated, and that the protein concentration had reached equilibrium. Actually the film had likely not completely reached saturation, although from the adsorption isotherm, it appears as though it may be near saturation. The monolayer antibody adsorption assumption for this model may be invalid, as multilayer models have been described in literature that varies the adsorption affinity slightly [138]. Increasing the initial concentration of antibody in solution may allow for the model to reach saturation and be further validated. Also important to note is the accuracy of the interferometer measurements may not be quite adequate for the scale of topographic features on the film. Another possible reason for inaccuracy is the variability between the surface topography between polymer films. This could result in higher surface area, thereby increasing antibody adsorption to the film compared to other films. The result of the antibody adsorption to CA/PMMA/PEO surfaces is system that will provide invalid results due to the inability of the gold-labeled antibodies to re-suspend and migrate along the length of the yarn.

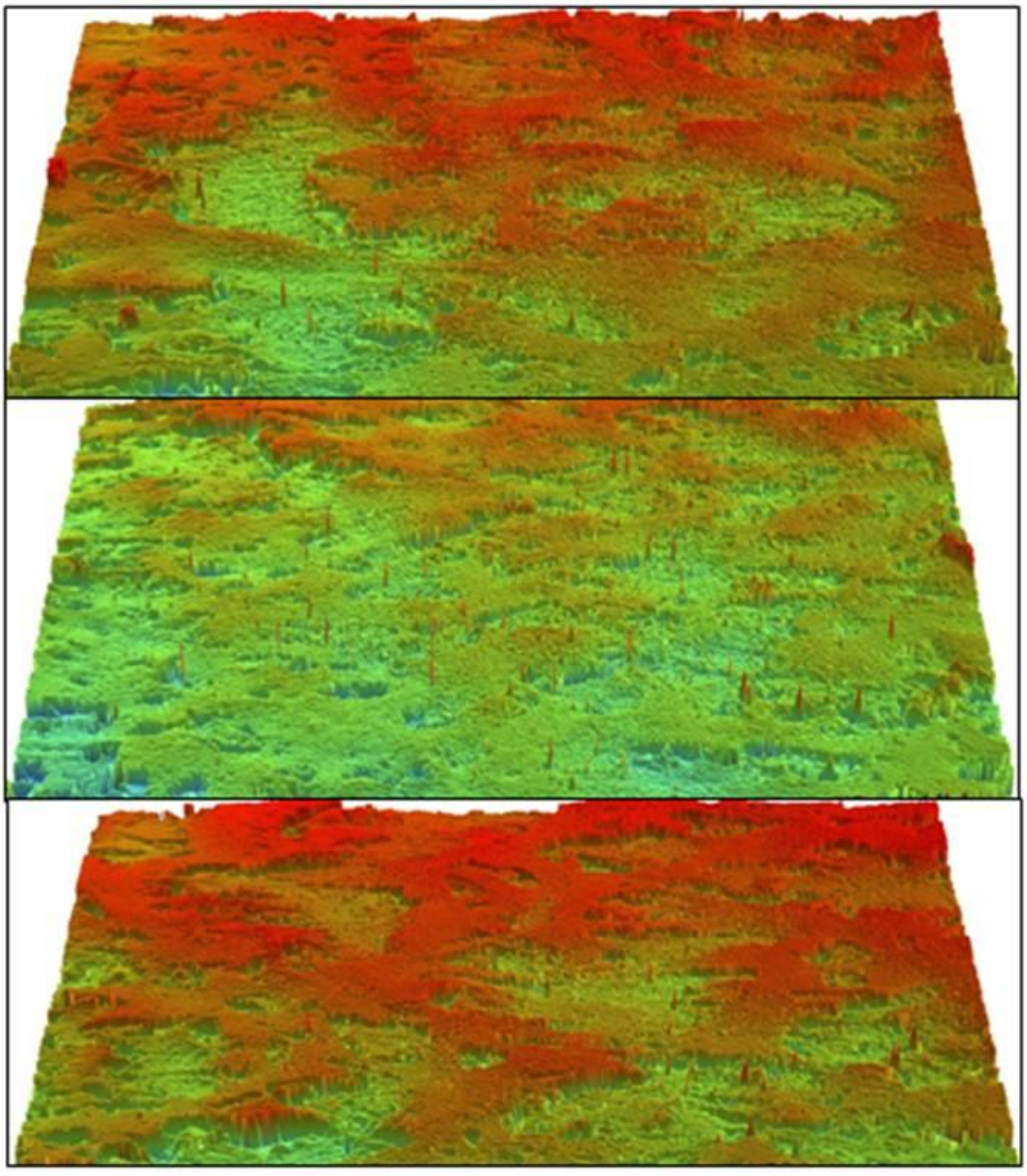

Figure 12.Three representative images captured by the interferometer. Each image is that of an average of 4.04 ± .01 mm^2 surface area which translates to 9.32± 0.31 mm^2 of actual surface area.

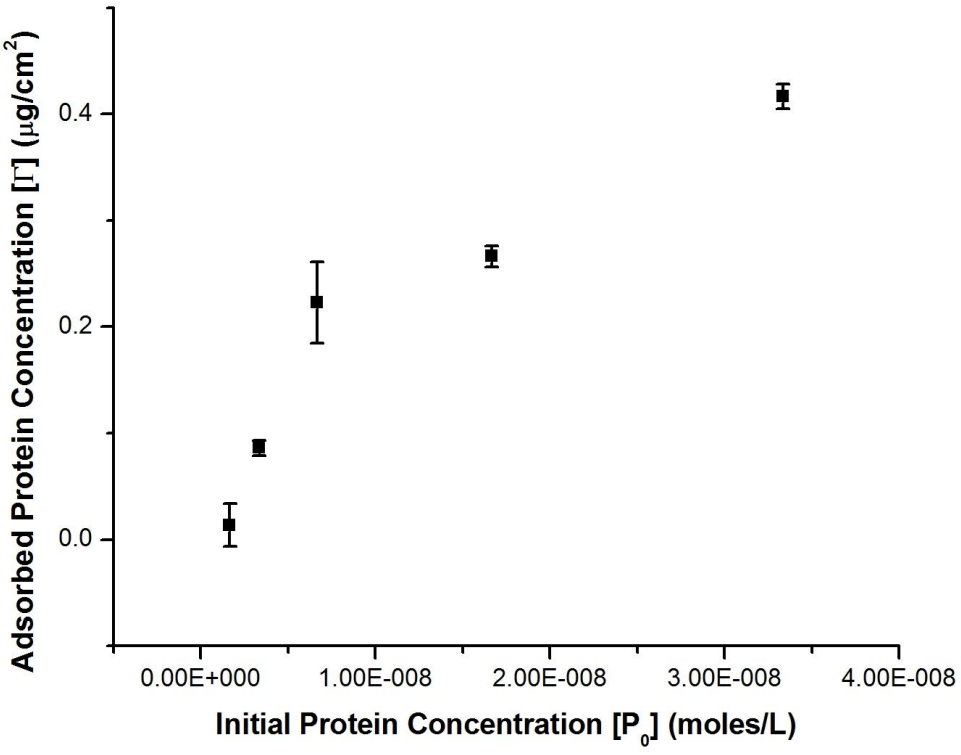

Figure 13. The antibody adsorption isotherm to the CA/PMMA/PEO films. It is apparent that increased protein concentration yields increased antibody adsorption. The films may have nearly reached saturation.

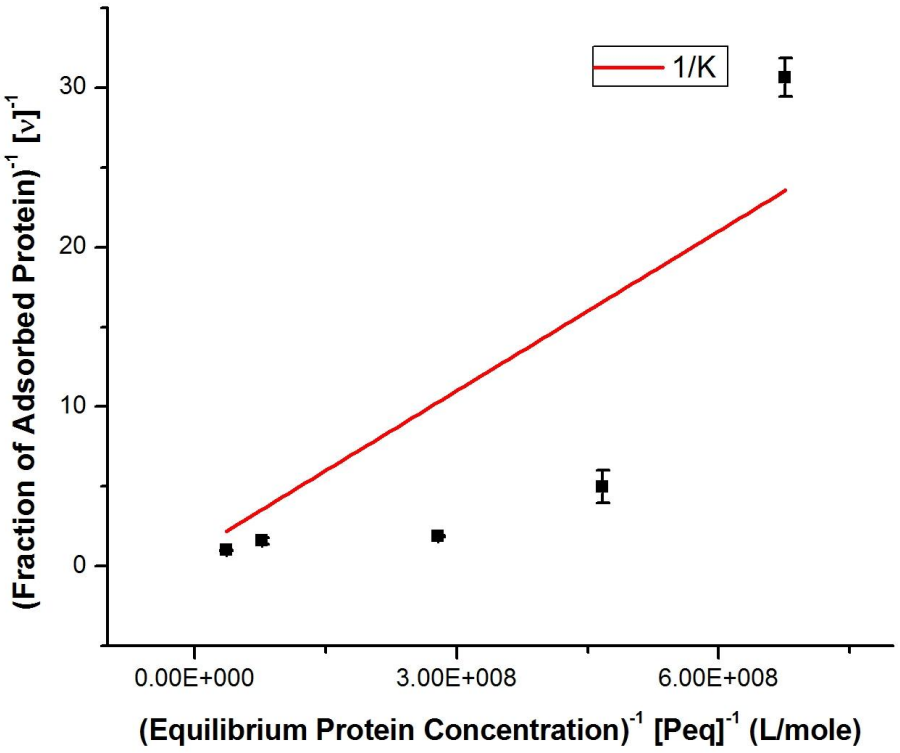

Figure 14. The plot of the equation $\mathbf{1}\ \boldsymbol{\nu} = (\mathbf{1}\ \boldsymbol{K})(\mathbf{1}\ [\boldsymbol{P_{eq}}]) + \mathbf{1}$ to determine the affinity constant for antibody adsorption. The affinity constant was found to be $3x10^7$, resulting in a Gibb's free energy of adsorption, $\Delta \boldsymbol{G} = \mathbf{-43}\ \pm \mathbf{0.3}\ \boldsymbol{kJ/mole}$. The adjusted R^2 value for the linear fit was 0.78.

Table 2. Results from the antibody adsorption experiment. Included are the Gibb's free energy, affinity constant and surface area of the films

Antibody Adsorption Results	
Film Surface Area (cm^2)	0.4
Affinity Constant [K]	$(3 \pm 0.4) \times 10^7$
Gibb's Free Energy of Adsorption [ΔG] (kJ/mole)	-43 ± 0.3

6.3.7 Conjugate Pad Contact Immunoassay

After wetting the gold nanoparticle conjugate pads with analyte solution and pressing them against the nanofiber yarn, gold nanoparticles quickly transferred from the low-retention glass fiber pads to the nanofiber yarns. The gold nanoparticles were wicked along the entire length of the immunoassay yarn and red coloration could be seen at 3 locations, as shown below in Figure 15.

Figure 15. Results of the contact conjugate pad immunoassay are shown here. Red coloration can be seen at 3 locations along the length of the yarn, the location of pressing the conjugate pad against the yarn (middle) and the location of the goat anti-rabbit IgG and rabbit anti-bovine IgG immobilization (left and right).

As a proof-of-concept that the nanoparticle conjugates dehydration procedure was effective and allowed for release from the conjugate pads to the immunoassay yarn, the contact conjugate pad immunoassay was performed. This system is less complex than the point-of-care system proposed earlier because fewer steps are performed by the end-user. The conjugate pad, which is pre-loaded with colloidal gold-labeled antibody, is dipped in the sample solution to be wetted, and then manually placed in contact against the immunoassay yarn. Rapid transfer of nanoparticle conjugates to the immunoassay yarn

was seen and results were evident in seconds. This procedure is very simple with accurate results and may be performed by patients as an in-home diagnostic tool, however simplification of the system would allow for less end-user error, whether the user is in a clinical laboratory or a patient at home. The clarity of the results was also needed to be improved to remove doubt and the possibility for misinterpretation by the end-user to meet CLIA-waived testing requirements.

The introduction of conjugate pads allowed for a two-component system where all the reagents were in a dried state, but did require some manual labor. This system is still procedurally more complex than current in-home diagnostic tests, such as pregnancy test [89, 90] and the OraQuick® in-home HIV test, yet have potential for employment in the in-home diagnostic market should the results be further clarified and easier to interpret. However, as is true for most products on the market in any industry, the simplest and most user-friendly products are much preferred by the consumer. To further simplify the process an immunoassay that requires only the addition of the sample, similar to the current LFIA in-home diagnostic tests, was pursued.

6.3.8 Conjugate Pad Incorporated Immunoassay Yarn

To make the procedure simpler for the end-user, the conjugate pad was incorporated into the yarn. The one-step system provided by the loaded conjugate pads twisted in the nanoparticle yarns achieved the simplicity of the current LFIA technology utilized in pregnancy tests [89, 90] and the OraQuick® HIV tests, by requiring the user only to add the sample to the conjugate pad location to obtain results. The results from the control

conjugate pad immunoassay are shown below in Figure 16. The immunoassay performed with the negative sample (goat anti-mouse IgG analyte) showed a very bright, sharp, and distinct nanoparticle accumulation at one stripe location. Red coloration can be seen at the location of the conjugate pad after sample addition and at the stripe of nanoparticle accumulation. After wicking excess, unbound nanoparticles away from the immunoassay yarn with a tissue by wicking, only the specific nanoparticle accumulation at the stripe remained.

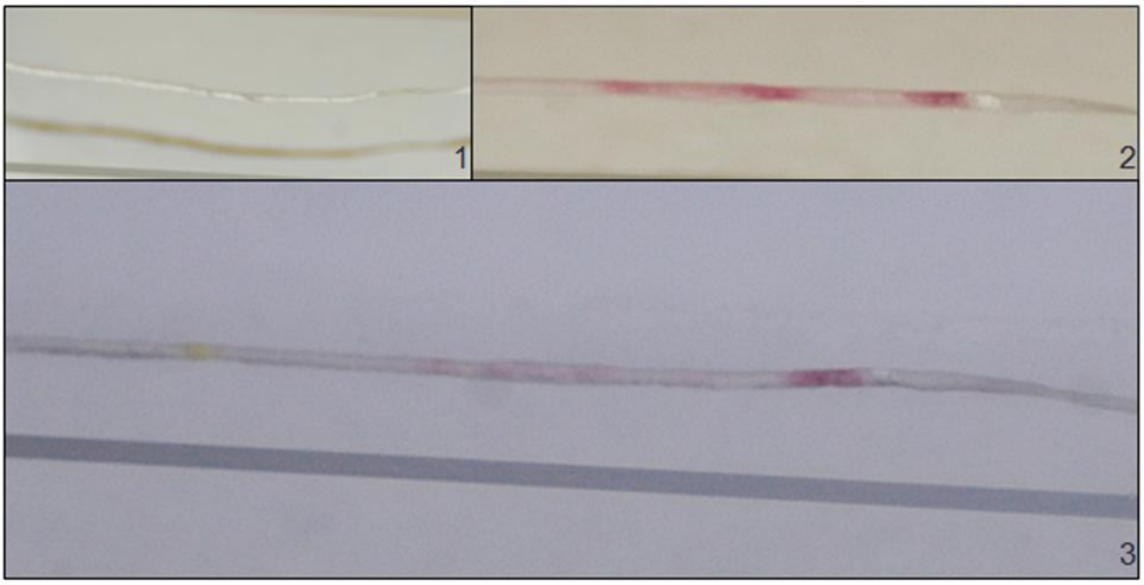

Figure 16. Results of the control immunoassay with the conjugate pad twisted in the center of the yarn. An immunoassay yarn after addition of a control sample with goat anti-mouse IgG (1 mg/ml) is shown. The immunoassay yarn is shown sequentially: before addition of sample (1), after addition of sample (2), and after wicking excess non-specifically bound nanoparticles via wicking (3).

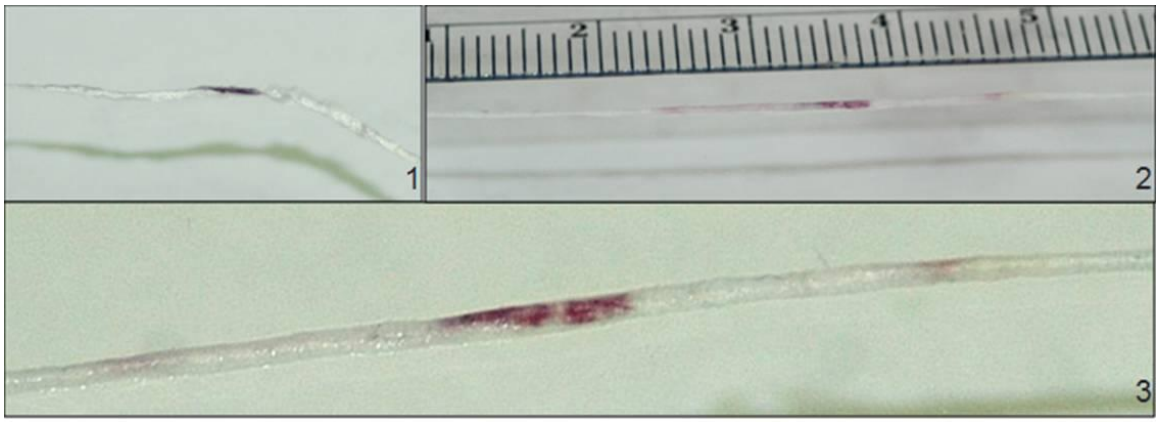

Figure 17. Results of the test analyte immunoassay with the conjugate pad twisted in the center of the yarn. An immunoassay after addition of a sample containing rabbit anti-bovine IgG (1 mg/ml) is shown. The immunoassay is shown sequentially: before the addition of sample (1), after addition of sample (2), and after wicking excess non-specifically bound nanoparticles via wicking (3).

The test sample containing the rabbit anti-bovine IgG analyte showed red coloration at the conjugate pad location as well as two stripes on either side approximately 1 cm from the each end of the conjugate pad, as shown in Figure 17.

The borosilicate glass fiber conjugate pads were then sectioned and cut to allow for twisting of the pads in the nanofiber yarns. The results are also clear and remove the possibility for misinterpretation by the end-user, as required to achieve CLIA-waived status and make the immunoassay feasible for patients to use as an in-home diagnostic tool. These immunoassay yarns could be marketed as is, however, to make the technology more attractive to the consumer implementation into a more polished final device or incorporation into a daily-use item such as facial tissue may increase the market-share captured. It is important to note that there was variability introduced to the

immunoassay yarn when twisting the conjugate pad in the middle of the yarn. Those with 50 µm sections of conjugate pads introduced fewer issues with uniform thickness and twist tightness. Additionally, conjugate pads placed in the exact center of the yarn thickness allowed for the best wicking of nanoparticles along the length of the immunoassay yarn to the test and control stripes.

6.3.9 Three Yarn System

The results of the three yarn system immunoassay are shown below in Figure 18. Red coloration can be seen on the test yarn and the positive control yarn, while the negative control yarn has less red coloration.

Figure 18. Three yarn system. The test yarn (left), positive control yarn (middle), and negative control yarn (right) after the immunoassay.

This system allows for a distinct result; however, there is skill involved at the same level as the analyte yarn system mentioned previously. This three yarn system may be more attractive to point-of-care facilities due to the additional confirmatory yarn that further validates results. It may also be twisted into a triple-yarn system for in-home diagnostics in the future or oriented in a geometric configuration, such as a triangle or a

parallel array, in daily use items such as facial tissues or panty liners. This would allow for patients to have immediate diagnosis of conditions, such as influenza and HIV, prior to symptom development. This would allow for the earliest possible detection of the condition.

6.3.10 Cost Analysis

A major advantage of the nanofiber-based immunoassay system is the potential for reduction in cost of manufacture of these devices for point-of-care and in-home use. This reduction in cost would increase the availability of the test to those with low income or in low-resource settings, such as third world countries and prison systems. Cost reduction may come from a reduction in the raw materials used and a cheaper manufacturing cost. The yarn systems will use fewer components. The sample pads and absorbent pads used in the current lateral flow immunoassay systems will not be used; the components will not require the plastic backing all the components are assembled on. Rather than use the nitrocellulose membranes, the yarn system will utilize the polymer yarns, which may be easier to manufacture. Smaller conjugate pads are used in the system allowing for cost saving as well. The conjugate pads employed in the yarn systems are 20 times thinner than with a 10 times smaller in the length and width dimensions. Table 2 provides a comparison between the current technology and the conjugate pad incorporated yarn system (the most expensive of these proposed systems) raw materials cost. Excluded from this analysis are the costs of the gold nanoparticles and antibodies. These costs would also be reduced due to the increased loading efficiency of the antibody on the

nanofiber yarns via covalent cross-linking. Packaging costs used in the analysis refer to the individual foil packaging of each current lateral flow immunoassay, which may not be necessary for the fiber system. The antibody estimate assumes that the fibers based system will allow for a 10% increase in antibody loading efficiency with the cross-linker from a 4-5 µg antibody loading. It is important to note that the cross-linker cost may be reduced with larger scale production. In addition to the raw materials savings, manufacturing cost are predicted to decrease due to the fewer components. Machinery will be eliminated, energy costs may be reduced, personnel costs would be reduced, and the time to manufacturing time should be reduced due to the fewer steps involved in component manufacture and assembly time. These factors combined lead to the potential for a cheaper diagnostic test platform that will increase availability, thus allowing more patients to seek the appropriate medical care.

Table 3. The raw materials cost comparison between the yarn system and the current lateral flow immunoassay yarn systems.

Component	**Cost ($) of Raw Materials Per Immunoassay**	
	Commercial LFIA	Yarn System
Yarn	0	0.04
Conjugate Pad	0.005	0.000025
Sample Pad	0.004	0
Nitrocellulose Membrane	0.009	0
Absorbent Pad	0.004	0
Plastic Backing	0.009	0
Cassette	0.4	0
HIV Antibody Estimate	11.88-14.85	10.69-13.37
Cross-linker	0	0.61
Total	**12.33-15.30**	**11.34-14.02**
Savings	-	**.99-1.28**

Chapter 7

Conclusions & Further Recommendations

7.1 Conclusions

It was determined that the CA/PMMA/PEO fiber composition was the best-suited for the application in an immunoassay yarn. This composition allows for sufficient antibody binding as determined by fluorescence microscopy. It also allows for sufficient wicking of the nanoparticle conjugates along the length of the yarn of any configuration.

The porosity and permeability of the yarns are appropriate to provide excellent wicking properties in our immunoassay system. While yarns of all compositions tested in this work allowed for sufficient antibody binding using the photo-reactive cross-linker, the CA/PMMA/PEO composition was the most appropriate for the wicking of the nanoparticle conjugates. The antibody immobilization technique also retained the antibody activity in the system with and without the streptavidin-biotin reaction. The gold nanoparticles offer appropriate size and antibody adsorption characteristics for employment in our immunoassay system.

The immunoassay systems developed throughout this work show promise for application in the field of diagnostics. The point-of-care system could be used in clinical

laboratories or at the point-of-care with minimal training. The gold nanoparticle conjugates cannot be loaded as a dry-reagent directly to the nanofibers, due to protein adsorption. This does not allow for the one-component system that is desired. However, borosilicate conjugate pads can be employed to simplify the procedure compared to the point-of-care immunoassay. The contact conjugate pad immunoassay system could also be employed in the clinical laboratory or point-of-care settings. A major void in the market is that of one-step, in-home diagnostic tests. The conjugate pad incorporated immunoassay system could be used as an in-home diagnostic tool, due to its ease of use and little chance for misinterpretation. The three yarn system could be used at the point-of-care and potentially employed for at home use. This system could also further reduce the cost of the immunoassay system by using fewer raw materials. The yarn systems also allow for greater than 10 times lower raw materials cost and potentially reduced manufacturing cost.

7.2 Further Recommendations

Wicking properties of the immunoassay yarns may be increased by increasing the hydrophilicity of the fibers. The sensitivity of the immunoassay system is extremely important to determine its successful employment as a diagnostic tool. Studies still need to be conducted on these systems to determine if clinically relevant analyte concentrations can be detected, as a model-system initially, and eventually using clinical samples. Should the current immunoassay method not be sufficient, introduction of the streptavidin-biotin system could increase the sensitivity efficiently. Silver-amplification

methods have also been shown effective in increasing the sensitivity of the immunochromatographic assays. This adds complexity and expense to the immunoassay, but may be a viable way to increase the sensitivity of the system for use in a clinical laboratory or point-of-care setting.

It is important to note that the increase of hydrophilicity may allow for an even simpler system, where there is no conjugate pad needed to release the nanoparticles. Increasing the hydrophilicity will more closely mimic the borosilicate glass fiber conjugate pad employed in the immunoassay. Incorporating poly(glycidyl methacrylate) (PGMA) or increasing the composition of PEO in the yarn may increase the hydrophilicity enough to lower the binding affinity of the yarn sufficiently and allow the nanoparticle conjugates to be dried on the nanofiber yarn in the same manner as they are dried on the conjugate pad. This will make the production of the immunoassay much simpler and may increase the wicking properties from the dried conjugate area, as the interfiber distances will be smaller without the disruption caused by the conjugate pad. This would also eliminate a component utilized in the immunoassay, reducing cost for the final product.

The point-of-care system and the contact conjugate pad system can be modified to be implemented in a high-throughput procedure. This would be advantageous for clinical laboratories that receive large volumes of samples for analysis to improve the turnaround time and diagnosis or confirmation for the patient. This could be accomplished by implementing manual devices similar to multi-channel pipettes and 96-well plates

commonly used for ELISA techniques. Automated equipment could also be implemented to enhance the amount of samples that can be analyzed. This would also reduce variability in results that may be obtained and eliminate the possibility of end-user error. After processing of the samples, the results could then be read by laboratory technicians to be reported back to the attending physicians and patients. The equipment required for this automated technique would only be appropriate for clinical laboratories that receive large quantities of samples for analysis from multiple centers for patient care.

Automated or higher-throughput preparation of the immunoassay yarns for point-of-care application, contact conjugate pad immunoassays, or in-home diagnostic tests should also be realized prior to marketing of the devices. This would decrease the possibility for variability between tests that may be introduced by different immunoassay production personnel or the same individual; thereby increasing quality and uniformity of the end-product.

Bibliography

1. Ozdemir, M.S., et al., *A label-free potentiometric sensor principle for the detection of antibody-antigen interactions.* Analytical Chemistry, 2013. **85**(9): p. 4770-6.

2. Hsu, J., et al., *Antivirals for Treatment of Influenza A Systematic Review and Meta-analysis of Observational Studies.* Annals of Internal Medicine, 2012. **156**(7): p. 512-U95.

3. Louie, J.K., et al., *Treatment With Neuraminidase Inhibitors for Critically Ill Patients With Influenza A (H1N1) pdm09.* Clinical Infectious Diseases, 2012. **55**(9): p. 1198-1204.

4. Siston, A.M., et al., *Pandemic 2009 Influenza A(H1N1) Virus Illness Among Pregnant Women in the United States.* Jama-Journal of the American Medical Association, 2010. **303**(15): p. 1517-1525.

5. Allwinn, R., et al., *Laboratory diagnosis of influenza - virology or serology?* Medical Microbiology and Immunology, 2002. **191**(3-4): p. 157-160.

6. Hsiung, G.D., *DIAGNOSTIC VIROLOGY - FROM ANIMALS TO AUTOMATION.* Yale Journal of Biology and Medicine, 1984. **57**(5): p. 727-733.

7. Leland, D.S. and C.C. Ginocchio, *Role of cell culture for virus detection in the age of technology.* Clinical Microbiology Reviews, 2007. **20**(1): p. 49-+.

8. Lee, G.-C., et al., *Evaluation of a rapid diagnostic test, NanoSign (R) Influenza A/B Antigen, for detection of the 2009 pandemic influenza A/H1N1 viruses.* Virology Journal, 2010. **7**.

9. *Guidance for Clinicians on the Use of Rapid Influenza Diagnostic Tests*, 2012, Centers for Disease Control and Prevention.

10. Vasoo, S., J. Stevens, and K. Singh, *Rapid Antigen Tests for Diagnosis of Pandemic (Swine) Influenza A/H1N1.* Clinical Infectious Diseases, 2009. **49**(7): p. 1090-1093.

11. Kim, D.-K. and B. Poudel, *Tools to Detect Influenza Virus.* Yonsei Medical Journal, 2013. **54**(3): p. 560-566.

12. Lucas, P.M., et al., *Diagnosis of 2009 Pandemic Influenza A (pH1N1) and Seasonal Influenza Using Rapid Influenza Antigen Tests, San Antonio, Texas, April-June 2009.* Clinical Infectious Diseases, 2011. **52**: p. S116-S122.

13. Al Johani, S.M., et al., *Validity of two rapid point of care influenza tests and direct fluorecence assay in comparison of real time PCR for swine of origin Influenza virus.* Journal of infection and public health, 2011. **4**(1): p. 7-11.

14. Farnham, P.G., et al., *Comparing the Costs of HIV Screening Strategies and Technologies in Health-Care Settings.* Public Health Reports, 2008. **123**: p. 51-62.

15. Shahar, E., et al., *Effect of HAART on Salivary Composition and Oxidative Profile in HIV-Infected Patients.* Current Hiv Research, 2008. **6**(5): p. 447-451.

16. Silva, A., et al., *Implementing an HIV and sexually transmitted disease screening program in an emergency department.* Annals of Emergency Medicine, 2007. **49**(5): p. 564-572.

17. Kurth, A.E., et al., *Clinician Practices and Attitudes Regarding Early Antiretroviral Therapy in the United States.* Jaids-Journal of Acquired Immune Deficiency Syndromes, 2012. **61**(5): p. E65-E69.

18. Mehta, S.D., et al., *Patient risks, outcomes, and costs of voluntary HIV testing at five testing sites within a medical center.* Public Health Reports, 2008. **123**(5): p. 608-617.

19. Phillips, K.A. and S. Fernyak, *The cost-effectiveness of expanded HIV counselling and testing in primary care settings: a first look.* Aids, 2000. **14**(14): p. 2159-2169.

20. Walensky, R.P., et al., *Effective HIV case identification through routine HIV screening at urgent care centers in Massachusetts.* American Journal of Public Health, 2005. **95**(1): p. 71-73.

21. Dee, K.C., D.A. Puleo, and R. Bizios, *An Introduction to Tissue-Biomaterial Interactions*2003: Wiley.

22. Alberts, B.J., A; Lewis, J.; et al., *Molecular Biology of the Cell, 4th edition*, 2002, Garland Science: New York.

23. Elgert, K.D., *Immunology: Understanding The Immune System*2009: Wiley.

24. Steward, M.W., *Antibodies: Their Structure and Functions*1984: Routledge, Chapman & Hall, Incorporated.

25. Harris, L.J., et al., *Refined structure of an intact IgG2a monoclonal antibody.* Biochemistry, 1997. **36**(7): p. 1581-1597.

26. F. C. Bernstein, T.F.K., G.J. Williams, E.E. Meyer Jr., M. D. Brice, J.R. Rodgers, O. Kennard, T. Shimanouchi, M. Tasumi, *The Protein Data Bank: A Computer-based Archival File for Macromolecular Structures.* J. of Mol. Biol., 1977. **112**.

27. Thomson, N.H., *The substructure of immunoglobulin G resolved to 25 kDa using amplitude modulation AFM in air.* Ultramicroscopy, 2005. **105**(1-4): p. 103-110.

28. Davies, D.R. and S. Chacko, *ANTIBODY STRUCTURE.* Accounts of Chemical Research, 1993. **26**(8): p. 421-427.

29. Wilson, L., P.T. Matsudaira, and D.J. Asai, *Antibodies in Cell Biology*1993: Elsevier Science.

30. Yuan, M., et al., *Computer-Aided Molecular Modeling Study on Antibody Recognition of Small Molecules: An Immunoassay for Triazine Herbicides.* Journal of Agricultural and Food Chemistry, 2012. **60**(42): p. 10486-10493.

31. Peters, T., et al., *Mouse model of foreign body reaction that alters the submesothelium and transperitoneal transport.* American Journal of Physiology-Renal Physiology, 2011. **300**(1): p. F283-F289.

32. Dalu, A., et al., *A comparison of the inflammatory response to a polydimethylsiloxane implant in male and female Balb/c mice.* Biomaterials, 2000. **21**(19): p. 1947-1957.

33. Raghavan, S.S., et al., *Human Flexor Tendon Tissue Engineering: Decellularization of Human Flexor Tendons Reduces Immunogenicity In Vivo.* Tissue Engineering Part A, 2012. **18**(7-8): p. 796-805.

34. Simionescu, A., et al., *Lectin and antibody-based histochemical techniques for cardiovascular tissue engineering.* Journal of Histotechnology, 2011. **34**(1): p. 20-28.

35. Lu, Q.J., et al., *Novel porous aortic elastin and collagen scaffolds for tissue engineering.* Biomaterials, 2004. **25**(22): p. 5227-5237.

36. Mercuri, J.J., S.S. Gill, and D.T. Simionescu, *Novel tissue-derived biomimetic scaffold for regenerating the human nucleus pulposus.* Journal of Biomedical Materials Research Part A, 2011. **96A**(2): p. 422-435.

37. Chuang, T.-H., et al., *Polyphenol-Stabilized Tubular Elastin Scaffolds for Tissue Engineered Vascular Grafts.* Tissue Engineering Part A, 2009. **15**(10): p. 2837-2851.

38. Both, L., et al., *Monoclonal antibodies for prophylactic and therapeutic use against viral infections.* Vaccine, 2013. **31**(12): p. 1553-1559.

39. Marasco, W.A. and J. Sui, *The growth and potential of human antiviral monoclonal antibody therapeutics.* Nature Biotechnology, 2007. **25**(12).

40. Webster, R.G., et al., *ANTIGENIC STRUCTURE AND VARIATION IN AN INFLUENZA VIRUS-N9 NEURAMINIDASE.* Journal of Virology, 1987. **61**(9): p. 2910-2916.

41. Webster, R.G. and W.G. Laver, *PREPARATION AND PROPERTIES OF ANTIBODY DIRECTED SPECIFICALLY AGAINST NEURAMINIDASE OF INFLUENZA VIRUS.* Journal of Immunology, 1967. **99**(1): p. 49-&.

42. Hultberg, A., et al., *Llama-Derived Single Domain Antibodies to Build Multivalent, Superpotent and Broadened Neutralizing Anti-Viral Molecules.* Plos One, 2011. **6**(4).

43. Imai, M., et al., *Fusion of influenza virus with the endosomal membrane is inhibited by monoclonal antibodies to defined epitopes on the hemagglutinin.* Virus Research, 1998. **53**(2): p. 129-139.

44. Krawczyk, A., et al., *Impact of Valency of a Glycoprotein B-Specific Monoclonal Antibody on Neutralization of Herpes Simplex Virus.* Journal of Virology, 2011. **85**(4): p. 1793-1803.

45. Pantophlet, R.A., *Antibody Epitope Exposure and Neutralization of HIV-1.* Current Pharmaceutical Design, 2010. **16**(33): p. 3729-3743.

46. Dykman, L.A. and V.A. Bogatyrev, *Gold nanoparticles: Preparation, functionalisation, applications in biochemistry and immunochemistry.* Uspekhi Khimii, 2007. **76**(2): p. 199-213.

47. Khlebtsov, B. and N. Khlebtsov, *Enhanced solid-phase immunoassay using gold nanoshells: effect of nanoparticle optical properties.* Nanotechnology, 2008. **19**(43).

48. Katoh, K., *Rapid fixation and immunofluorescent staining of cultured cells using microwave irradiation.* Journal of Histotechnology, 2011. **34**(1): p. 29-34.

49. McMullen, R.L., et al., *Image analysis to quantify histological and immunofluorescent staining of ex vivo skin and skin cell cultures.* International Journal of Cosmetic Science, 2010. **32**(2): p. 143-154.

50. Yu, B., Y.J. Liu, and X. Yin, *Elimination of non-specific staining in immunohistochemistry of human liver tissues by modulation of antibody-antigen binding microenvironment.* Journal of Histotechnology, 2013. **36**(1): p. 3-10.

51. Chou, S.-F., *Development of a manual self-assembled colloidal gold nanoparticle-immunochromatographic strip for rapid determination of human interferon-gamma.* Analyst, 2013. **138**(9): p. 2620-2623.

52. van der Loos, C.M., et al., *Immunohistochemical detection of interferon-gamma: Fake or fact?* Journal of Histochemistry & Cytochemistry, 2001. **49**(6): p. 699-709.

53. Butler, J.E., et al., *The immunochemistry of sandwich ELISAs: VI. Greater than 90 percent of monoclonal and 75 percent of polyclonal anti-fluorescyl capture antibodies (CAbs) are denatured by passive adsorption.* Molecular Immunology, 1993. **30**(13): p. 1165-1175.

54. Linares, E.M., et al., *Enhancement of the detection limit for lateral flow immunoassays: Evaluation and comparison of bioconjugates.* Journal of Immunological Methods, 2012. **375**(1-2): p. 264-270.

55. Salomone, A., et al., *Reliability of detection of Citrus tristeza virus by an immunochromatographic lateral flow assay in comparison with ELISA.* Journal of Plant Pathology, 2004. **86**(1): p. 43-48.

56. Song, H.-O., et al., *Polymeric LabChip Real-Time PCR as a Point-of-Care-Potential Diagnostic Tool for Rapid Detection of Influenza A/H1N1 Virus in Human Clinical Specimens.* Plos One, 2012. **7**(12).

57. Yu, H., et al., *Risk Factors for Severe Illness with 2009 Pandemic Influenza A (H1N1) Virus Infection in China.* Clinical Infectious Diseases, 2011. **52**(4): p. 457-465.

58. Prevention, C.f.D.C.a., *space HIV Testing Implementation Guidance for Correctional Settings*, V.H. National Center for HIV/AIDS, STD, and TB Prevention, Editor 2009.

59. Administration, U.S.F.a.D., *Device Advice: Comprehensive Regulatory Assistance*, 2009.

60. *Code of Federal Regulations Title 42, part 493*.

61. Agoritsas, K., et al., *Evaluation of the Quidel QuickVue test for detection of influenza A and B viruses in the pediatric emergency medicine setting by use of three specimen collection methods.* Journal of Clinical Microbiology, 2006. **44**(7): p. 2638-2641.

62. Cheng, X.-D., et al., *Evaluation of a new rapid influenza A diagnostic test for detection of pandemic (H1N1) 2009 and seasonal influenza A virus.* Journal of Clinical Virology, 2011. **50**(2): p. 153-155.

63. Loens, K., et al., *Optimal Sampling Sites and Methods for Detection of Pathogens Possibly Causing Community-Acquired Lower Respiratory Tract Infections.* Journal of Clinical Microbiology, 2009. **47**(1): p. 21-31.

64. Irwin, R.S. and J.M. Rippe, *Irwin and Rippe's intensive care medicine*2008: Wolters Kluwer Health/Lippincott Williams & Wilkins.

65. Harper, S.A., et al., *Seasonal Influenza in Adults and Children-Diagnosis, Treatment, Chemoprophylaxis, and Institutional Outbreak Management: Clinical Practice Guidelines of the Infectious Diseases Society of America.* Clinical Infectious Diseases, 2009. **48**(8): p. 1003-1032.

66. Centers for Disease, C. and Prevention, *Evaluation of rapid influenza diagnostic tests for detection of novel influenza A (H1N1) Virus - United States, 2009.* MMWR. Morbidity and mortality weekly report, 2009. **58**(30): p. 826-9.

67. Lucas, A. and B. Armbruster, *The cost-effectiveness of expanded HIV screening in the United States.* Aids, 2013. **27**(5): p. 795-801.

68. McNaghten, A.D., et al., *Routine HIV Testing among Providers of HIV Care in the United States, 2009.* Plos One, 2013. **8**(1).

69. Beckwith, C.G., et al., *Feasibility and acceptability of rapid HIV testing in jail.* Aids Patient Care and Stds, 2007. **21**(1): p. 41-47.

70. MacGowan, R., et al., *Voluntary Rapid Human Immunodeficiency Virus (HIV) Testing in Jails.* Sexually Transmitted Diseases, 2009. **36**(2): p. S9-S13.

71. Weinbaum, C.A., K.M. Sabin, and S.S. Santibanez, *Hepatitis B, hepatitis C, and HIV in correctional populations: a review of epidemiology and prevention.* Aids, 2005. **19**: p. S41-S46.

72. *OraQuick(R) In-Home HIV Test Summary of Safety and Effectiveness. PMA BP120001*, F.a.D. Administration, Editor.

73. Byzova, N.A., et al., *Immunochromatographic Assay with Photometric Detection for Rapid Determination of the Herbicide Atrazine and Other Triazines in Foodstuffs.* Journal of Aoac International, 2010. **93**(1): p. 36-43.

74. Delmulle, B.S., et al., *Development of an immunoassay-based lateral flow dipstick for the rapid detection of aflatoxin B-1 in pig feed.* Journal of Agricultural and Food Chemistry, 2005. **53**(9): p. 3364-3368.

75. Gas, F., et al., *One step immunochromatographic assay for the rapid detection of Alexandrium minutum.* Biosensors & Bioelectronics, 2010. **25**(5): p. 1235-1239.

76. Li, Y., et al., *Development of a convenient immunochromatographic strip for the diagnosis of infection with Japanese encephalitis virus in swine.* Journal of Virological Methods, 2010. **168**(1-2): p. 51-56.

77. Mao, X., et al., *Disposable Nucleic Acid Biosensors Based on Gold Nanoparticle Probes and Lateral Flow Strip.* Analytical Chemistry, 2009. **81**(4): p. 1660-1668.

78. Xu, H., et al., *Aptamer-Functionalized Gold Nanoparticles as Probes in a Dry-Reagent Strip Biosensor for Protein Analysis.* Analytical Chemistry, 2009. **81**(2): p. 669-675.

79. Yu, C.Y., et al., *Dry-reagent gold nanoparticle-based lateral flow biosensor for the simultaneous detection of Vibrio cholerae serogroups O1 and O139.* Journal of Microbiological Methods, 2011. **86**(3): p. 277-282.

80. Zhang, M.-Z., et al., *Development of a colloidal gold-based lateral-flow immunoassay for the rapid simultaneous detection of clenbuterol and ractopamine in swine urine.* Analytical and Bioanalytical Chemistry, 2009. **395**(8): p. 2591-2599.

81. Kolosova, A.Y., et al., *Development of a colloidal gold-based lateral-flow immunoassay for the rapid simultaneous detection of zearalenone and deoxynivalenol.* Analytical and Bioanalytical Chemistry, 2007. **389**(7-8): p. 2103-2107.

82. Saleh, M., et al., *Antibody-coated gold nanoparticles immunoassay for direct detection of Aeromonas salmonicida in fish tissues.* Journal of Fish Diseases, 2011. **34**(11): p. 845-852.

83. Duan, C.-F., Y.-Q. Yu, and H. Cui, *Gold nanoparticle-based immunoassay by using non-stripping chemiluminescence detection.* Analyst, 2008. **133**(9): p. 1250-1255.

84. Monk, D.J. and D.R. Walt, *Optical fiber-based biosensors.* Analytical and Bioanalytical Chemistry, 2004. **379**(7-8): p. 931-945.

85. Penn, S.G., L. He, and M.J. Natan, *Nanoparticles for bioanalysis.* Current Opinion in Chemical Biology, 2003. **7**(5): p. 609-615.

86. Thanh, N.T.K. and Z. Rosenzweig, *Development of an aggregation-based immunoassay for anti-protein A using gold nanoparticles.* Analytical Chemistry, 2002. **74**(7): p. 1624-1628.

87. Rojanathanes, R., et al., *GOLD NANOPARTICLE AS AN ALTERNATIVE TOOL FOR A URINE PREGNANCY TEST.* Taiwanese Journal of Obstetrics & Gynecology, 2008. **47**(3): p. 296-299.

88. Posthuma-Trumpie, G.A., J. Korf, and A. van Amerongen, *Lateral flow (immuno) assay: its strengths, weaknesses, opportunities and threats. A literature survey.* Analytical and Bioanalytical Chemistry, 2009. **393**(2): p. 569-582.

89. Cole, L.A., *The hCG assay or pregnancy test.* Clinical Chemistry and Laboratory Medicine, 2012. **50**(4): p. 617-630.

90. Cole, L.A., et al., *Sensitivity of over-the-counter pregnancy tests: Comparison of utility and marketing messages.* Journal of the American Pharmacists Association, 2005. **45**(5): p. 608-615.

91. Old, J.B., et al., *Developmental Validation of RSID (TM)-Saliva: A Lateral Flow Immunochromatographic Strip Test for the Forensic Detection of Saliva.* Journal of Forensic Sciences, 2009. **54**(4): p. 866-873.

92. Aldus, C.F., et al., *Principles of some novel rapid dipstick methods for detection and characterization of verotoxigenic Escherichia coli.* Journal of Applied Microbiology, 2003. **95**(2): p. 380-389.

93. Verheijen, R., et al., *Development of a one step strip test for the detection of (dihydro)streptomycin residues in raw milk.* Food and Agricultural Immunology, 2000. **12**(1): p. 31-40.

94. Wang, S., et al., *Rapid determination of fumonisin B-1 in food samples by enzyme-linked Immunosorbent assay and colloidal gold immunoassay.* Journal of Agricultural and Food Chemistry, 2006. **54**(7): p. 2491-2495.

95. Wang, X., et al., *Development of an immunochromatographic lateral-flow test strip for rapid detection of sulfonamides in eggs and chicken muscles.* Journal of Agricultural and Food Chemistry, 2007. **55**(6): p. 2072-2078.

96. Zhang, C., Y. Zhang, and S. Wang, *Development of multianalyte flow-through and lateral-flow assays using gold particles and horseradish peroxidase as tracers for the rapid determination of carbaryl and endosulfan in agricultural products.* Journal of Agricultural and Food Chemistry, 2006. **54**(7): p. 2502-2507.

97. Kim, Y.M., et al., *Development of an ultrarapid one-step fluorescence immunochromatographic assay system for the quantification of microcystins.* Environmental Science & Technology, 2003. **37**(9): p. 1899-1904.

98. Luo, Y., et al., *Novel Biosensor Based on Electrospun Nanofiber and Magnetic Nanoparticles for the Detection of E. coli O157:H7.* Ieee Transactions on Nanotechnology, 2012. **11**(4): p. 676-681.

99. Alves, N.J., T. Kiziltepe, and B. Bilgicer, *Oriented Surface Immobilization of Antibodies at the Conserved Nucleotide Binding Site for Enhanced Antigen Detection.* Langmuir, 2012. **28**(25): p. 9640-9648.

100. Butler, J.E., et al., *THE PHYSICAL AND FUNCTIONAL-BEHAVIOR OF CAPTURE ANTIBODIES ADSORBED ON POLYSTYRENE.* Journal of Immunological Methods, 1992. **150**(1-2): p. 77-90.

101. Blencowe, A. and W. Hayes, *Development and application of diazirines in biological and synthetic macromolecular systems.* Soft Matter, 2005. **1**(3): p. 178-205.

102. Collioud, A., et al., *ORIENTED AND COVALENT IMMOBILIZATION OF TARGET MOLECULES TO SOLID SUPPORTS - SYNTHESIS AND APPLICATION OF A LIGHT-ACTIVATABLE AND THIOL-REACTIVE CROSS-LINKING REAGENT.* Bioconjugate Chemistry, 1993. **4**(6): p. 528-536.

103. Dankbar, D.M. and G. Gauglitz, *A study on photolinkers used for biomolecule attachment to polymer surfaces.* Analytical and Bioanalytical Chemistry, 2006. **386**(7-8): p. 1967-1974.

104. Liu, X.H., et al., *Photopatterning of antibodies on biosensors.* Bioconjugate Chemistry, 2000. **11**(6): p. 755-761.

105. Miller, J.C., et al., *Antibody microarray profiling of human prostate cancer sera: Antibody screening and identification of potential biomarkers.* Proteomics, 2003. **3**(1): p. 56-63.

106. Sigrist, H., et al., *SURFACE IMMOBILIZATION OF BIOMOLECULES BY LIGHT.* Optical Engineering, 1995. **34**(8): p. 2339-2348.

107. Kausaite-Minkstimiene, A., et al., *Comparative Study of Random and Oriented Antibody Immobilization Techniques on the Binding Capacity of Immunosensor.* Analytical Chemistry, 2010. **82**(15): p. 6401-6408.

108. Brunner, J., H. Senn, and F.M. Richards, *"3-TRIFLUOROMETHYL-3-PHENYLDIAZIRINE - A NEW CARBENE GENERATING GROUP FOR PHOTOLABELING REAGENTS.* Journal of Biological Chemistry, 1980. **255**(8): p. 3313-3318.

109. Scientific, T. *Photoreactive Crosslinker Chemistry*. Available from: http://www.piercenet.com/browse.cfm?fldID=F3324640-A85B-7AB2-CBB8-CFD7065F70C6.

110. Bai, Y., et al., *Aptamer/thrombin/aptamer-AuNPs sandwich enhanced surface plasmon resonance sensor for the detection of subnanomolar thrombin.* Biosensors & Bioelectronics, 2013. **47**: p. 265-70.

111. Moelans, C.B., et al., *Current technologies for HER2 testing in breast cancer.* Critical Reviews in Oncology Hematology, 2011. **80**(3): p. 380-392.

112. Tsai, C.-C., et al., *Nanoporous artificial proboscis for probing minute amount of liquids.* Nanoscale, 2011. **3**(11): p. 4685-4695.

113. Callegari, G., et al., *Absorption and transport properties of ultra-fine cellulose webs.* Journal of Colloid and Interface Science, 2011. **353**(1): p. 290-293.

114. Rahli, O., et al., *Fluid flow through randomly packed monodisperse fibers: The Kozeny-Carman parameter analysis.* Journal of Fluids Engineering-Transactions of the Asme, 1997. **119**(1): p. 188-192.

115. Mei, Y., et al., *Electrostatic polarization is critical for the strong binding in streptavidin-biotin system.* Journal of Computational Chemistry, 2012. **33**(15): p. 1374-1382.

116. Bykhovski, A., et al., *Analysis of Electronic Structure, Binding, and Vibrations in Biotin-Streptavidin Complexes Based on Density Functional Theory and Molecular Mechanics.* Journal of Physical Chemistry B, 2013. **117**(1): p. 25-37.

117. Sreenivasan, V.K.A., et al., *A modular design of low-background bioassays based on a high-affinity molecular pair barstar:barnase.* Proteomics, 2013. **13**(9): p. 1437-1443.

118. Doyen, M., K. Bartik, and G. Bruylants, *UV-Vis and NMR study of the formation of gold nanoparticles by citrate reduction: Observation of gold-citrate aggregates.* Journal of Colloid and Interface Science, 2013. **399**: p. 1-5.

119. Turkevich, J., P.C. Stevenson, and J. Hillier, *A Study of the Nucleation and Growth processes in the Synthesis of Colloidal Gold.* Discussions of the Faraday Society, 1951. **11**: p. 55-75.

120. Chow, M.K. and C.F. Zukoski, *GOLD SOL FORMATION MECHANISMS - ROLE OF COLLOIDAL STABILITY.* Journal of Colloid and Interface Science, 1994. **165**(1): p. 97-109.

121. Ji, X., et al., *Size control of gold nanocrystals in citrate reduction: The third role of citrate.* Journal of the American Chemical Society, 2007. **129**(45): p. 13939-13948.

122. Pong, B.-K., et al., *New insights on the nanoparticle growth mechanism in the citrate reduction of Gold(III) salt: Formation of the au nanowire intermediate and its nonlinear optical properties.* Journal of Physical Chemistry C, 2007. **111**(17): p. 6281-6287.

123. Hayat, A., *Colloidal gold: principles, methods, and applications*1989: Academic Press.

124. Jeong, H.-H., et al., *Real-time label-free immunoassay of interferon-gamma and prostate-specific antigen using a Fiber-Optic Localized Surface Plasmon Resonance sensor.* Biosensors & Bioelectronics, 2013. **39**(1): p. 346-351.

125. Zabetakis, K., et al., *Effect of high gold salt concentrations on the size and polydispersity of gold nanoparticles prepared by an extended Turkevich-Frens method.* Gold Bulletin, 2012. **45**(4): p. 203-211.

126. Zhao, P., N. Li, and D. Astruc, *State of the art in gold nanoparticle synthesis.* Coordination Chemistry Reviews, 2013. **257**(3-4): p. 638-665.

127. Nakamoto, K.T., et al., *ANALYSIS OF EXCITATORY SYNAPSES IN THE GUINEA PIG INFERIOR COLLICULUS: A STUDY USING ELECTRON MICROSCOPY AND GABA IMMUNOCYTOCHEMISTRY.* Neuroscience, 2013. **237**: p. 170-183.

128. Scala, G. and L. Maruccio, *Angiogenesis of buffalo choroid plexuses: Structural and immunocytochemical study.* Microscopy Research and Technique, 2012. **75**(8): p. 1104-1112.

129. Hermanson, G.T., *Bioconjugate Techniques*1996: Elsevier Science.

130. Aurion, *Aurion Gold Sol Technical Data Sheet.*

131. Konwarh, R., N. Karak, and M. Misra, *Electrospun cellulose acetate nanofibers: The present status and gamut of biotechnological applications.* Biotechnology advances, 2013. **31**(4): p. 421-37.

132. Hardick, O., et al., *Nanofiber adsorbents for high productivity downstream processing.* Biotechnology and Bioengineering, 2013. **110**(4): p. 1119-1128.

133. Sundarrajan, S., et al., *Potential of Engineered Electrospun Nanofiber Membranes for Nanofiltration Applications.* Drying Technology, 2013. **31**(2): p. 163-169.

134. Reukov, V., et al., *Fabrication of nanocoated fibers for self-diagnosis of bacterial vaginosis.* Materials Science & Engineering C-Biomimetic and Supramolecular Systems, 2009. **29**(3): p. 669-673.

135. Vatansever, F., et al., *Toward Fabric-Based Flexible Microfluidic Devices: Pointed Surface Modification for pH Sensitive Liquid Transport.* Acs Applied Materials & Interfaces, 2012. **4**(9): p. 4541-4548.

136. Coskuntuna, E., A.J. Fowler, and S.B. Warner, *Fibrous structures with designed wicking properties.* Textile Research Journal, 2007. **77**(4): p. 256-264.

137. Owens, T.L., et al., *Control of Microfluidic Flow in Amphiphilic Fabrics.* Acs Applied Materials & Interfaces, 2011. **3**(10): p. 3796-3803.

138. Beeskow, T., K.H. Kroner, and F.B. Anspach, *Nylon-based affinity membranes: Impacts of surface modification on protein adsorption.* Journal of Colloid and Interface Science, 1997. **196**(2): p. 278-291.